

6. BASEMENT GEOCHEMISTRY, HOLE 504B¹

Rolf Emmermann, Mineralogisch-Petrologisches Institut, Justus-Liebig-Universität²

ABSTRACT

DSDP Hole 504B is the deepest section drilled into oceanic basement, penetrating through a 571.5-m lava pile and a 209-m transition zone of lavas and dikes into 295 m of a sheeted dike complex. To define the basement composition 194 samples of least altered basalts, representing all lithologic units, were analyzed for their major and 26 trace elements. As is evident from the alteration-sensitive indicators H_2O^+ , CO_2 , S, K, Mn, Zn, Cu, and the iron oxidation ratio, all rocks recovered are chemically altered to some extent. Downhole variation in these parameters enables us to distinguish five depth-related alteration zones that closely correlate with changes in alteration mineralogy. Alteration in the uppermost basement portion is characterized by pronounced K-uptake, sulfur loss, and iron oxidation and clearly demonstrates low-temperature seawater interaction. A very spectacular type of alteration is confined to the depth range from 910 to 1059 m below seafloor (BSF). Rocks from this basement portion exhibit the lowest iron oxidation, the highest H_2O^+ contents, and a considerable enrichment in Mn, S, Zn, and Cu. At the top of this zone a stockwork-like sulfide mineralization occurs. The chemical data suggest that this basement portion was at one time within a hydrothermal upflow zone. The steep gradient in alteration chemistry above this zone and the ore precipitation are interpreted as the result of mixing of the upflowing hydrothermal fluids with lower-temperature solutions circulating in the lava pile.

Despite the chemical alteration the primary composition and variation of the rocks can be reliably established. All data demonstrate that the pillow lavas and the dikes are remarkably uniform and display almost the same range of variation. A general characteristic of the rocks that classify as olivine tholeiites is their high MgO contents (up to 10.5 wt. %) and their low K abundances (~200 ppm). According to their mg-values, which range from 0.60 to 0.74, most basalts appear to have undergone some high-level crystal fractionation. Despite the overall similarity in composition, there are two major basalt groups that have significantly different abundances and ratios of incompatible elements at similar mg-values. The majority of the basalts from the pillow lava and dike sections are chemically closely related, and most probably represent differentiation products of a common parental magma. They are low in Na_2O , TiO_2 , and P_2O_5 , and very low in the more hygromagmaphile elements. Interdigitated with this basalt group is a very rarely occurring basalt that is higher in Na_2O , TiO_2 , P_2O_5 , much less depleted in hygromagmaphile elements, and similar to normal mid-ocean ridge basalt (MORB). The latter is restricted to Lithologic Units 5 and 36 of the pillow lava section and Lithologic Unit 83 of the dike section. The two basalt groups cannot be related by differentiation processes but have to be regarded as products of two different parental magmas. The compositional uniformity of the majority of the basalts suggests that the magma chamber beneath the Costa Rica Rift reached nearly steady-state conditions. However, the presence of lavas and dikes that crystallized from a different parental magma requires the existence of a separate conduit-magma chamber system for these melts. Occasionally mixing between the two magma types appears to have occurred. The chemical characteristics of the two magma types imply some heterogeneity in the mantle source underlying the Costa Rica Rift. The predominant magma type represents an extremely depleted source, whereas the rare magma type presumably originated from regions of less depleted mantle material (relict or affected by metasomatism).

INTRODUCTION: THE BASEMENT AT SITE 504

Hole 504B, which is located in 5.9-m.y.-old crust some 200 km south of the Costa Rica Rift, has established the longest section through oceanic layer 2 that has yet been drilled. It was cored by the joint effort of three DSDP Legs (69, 70, and 83) to a total depth of 1350 m BSF; 1075.5 m were into the basaltic basement. Basement recovery was 224 m, corresponding to an average of 20.8%.

The lithostratigraphic sequence in this hole is shown schematically in Figure 1. Since young crust on the southern flank of the Costa Rica Rift passes through the equatorial high productivity zone, there accumulated at this site a sedimentary blanket, 274.5 m thick, which effectively sealed the underlying basaltic crust from open circulation of seawater, that is, from convective heat loss. Measured heat flow, therefore, falls close to the theoretical curve for conductive cooling of ocean crust.

The temperature measured on Leg 69 at the basement/sediment interface was 60°C, and the maximum temperature obtained at the bottom of the hole at the end of Leg 83 was 135°C, corresponding to about 160°C after thermal disturbance by drilling has decayed (Becker et al., this volume).

Stratigraphically, the basement cored at Site 504 can be divided into three zones (Fig. 1). The upper 571.5 m, that is, down to 846 m BSF, are made up of pillow basalts and brecciated pillow material with some interlayered thin lava flows (1 to 2 m) and occasional intercalations of massive cooling units up to 15 m thick. This upper zone (volcanic layer) is underlain by a 209-m transition zone (down to 1055 m BSF) which consists of pillow basalts, massive units, and dikes, the latter becoming progressively more abundant with depth. Below 1055 m BSF (= 780 m sub-basement) no more pillows were identified. This depth was, therefore, chosen as the upper boundary of the lowermost zone, which is composed solely of dikes and massive cooling units and which is interpreted as part of a sheeted dike complex (Anderson et al., 1982; Adamson, this volume).

¹ Anderson, R. N., Honnorez, J., Becker, K., et al., *Init. Repts. DSDP*, 83: Washington (U.S. Govt. Printing Office).

² Address: Mineralogisch-Petrologisches Institut, Justus-Liebig-Universität, Senckenbergstr. 3, 6300 Giessen, Federal Republic of Germany.

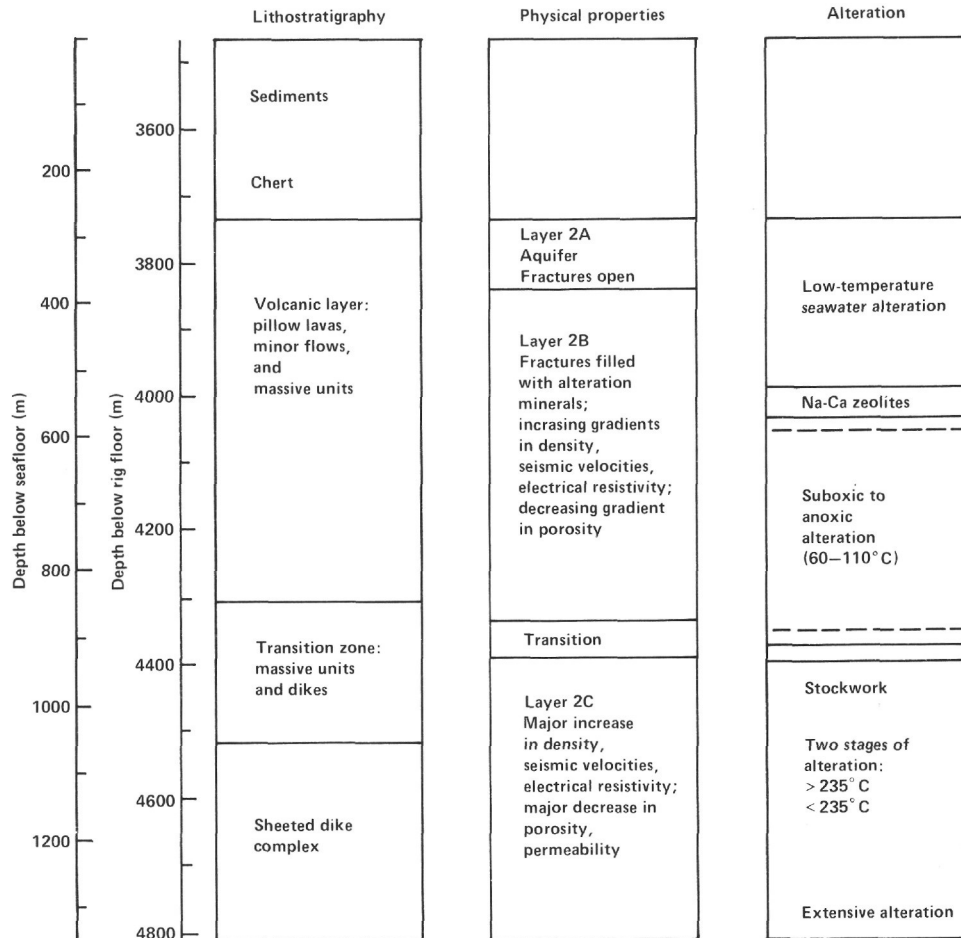


Figure 1. Downhole changes in lithostratigraphy, physical basement properties, and alteration.

The majority of the lithologic units of the volcanic section are made up of aphyric to moderately plagioclase-olivine phyric basalts that occasionally contain clumps of plagioclase and augite. Less common petrographic types are plagioclase-olivine phyric basalts with accessory chrome-spinel phenocrysts and highly phyric (10–20% phenocrysts) basalts carrying emerald green clinopyroxene phenocrysts as well as plagioclase and olivine. The estimated abundance of basaltic lithologies recovered from the transition zone and dike section is 40% aphyric, 29% sparsely to moderately plagioclase-olivine-clinopyroxene phyric, 18% plagioclase-olivine ± clinopyroxene phyric with accessory chrome-spinel, and 13% plagioclase-olivine phyric.

All rocks recovered are altered to some extent, although fresh basaltic glass was encountered in pillow rims down to about 800 m BSF. From the downhole variation in secondary minerals and mineral assemblages three depth-related alteration zones have been established (Fig. 1). Alteration from the basalt/sediment interface down to 584.5 m BSF corresponds to the “seafloor weathering” commonly observed in DSDP holes and is interpreted as the result of two superimposed stages of low-temperature alteration: an earlier stage of oxidative alteration followed by a later stage of suboxic to anoxic alteration (Honnorez et al., 1983). This “upper

alteration zone” is characterized by the presence of iron hydroxides and celadonite-nontronite that fill voids and replace olivine. A localized (Na and Na-Ca) zeolite alteration zone occurs superimposed in a narrow interval between 528.5 and 563 m BSF. Below 584.5 m, down to 836 m, only anoxic alteration, either with seawater at low water/rock ratios or with seawater that had previously reacted with basalt, occurred (“lower alteration zone”). Characteristic secondary minerals are saponite and pyrite, as well as minor calcite, quartz, Na zeolites, and anhydrite (Alt et al., this volume). Temperatures of alteration throughout the pillow section were probably less than 100°C, although the zeolite zone may have formed at slightly higher temperatures (Honnorez et al., 1983). Alteration of the lowermost 10 m of the volcanic section and the upper portion of the transition zone (836 m to 898 m BSF) is similar to that of the lower alteration zone but most probably took place at temperatures above 100°C (Alt et al., this volume). A third alteration zone which is characterized by greenschist and superimposed zeolite-facies mineral parageneses extends from 898 m down to the bottom of the hole. Among the characteristic secondary minerals are chlorite, actinolite, albite, epidote, sphene, analcite, and laumontite. Between 911 and 928 m BSF, within the transition zone, a mineralized stockwork-like zone was recovered where

pyrite, sphalerite, chalcopyrite, and minor galena occur in veins in a highly altered pillow sequence.

According to the large number of geophysical experiments and measurements conducted during Leg 83 there is also a very pronounced downhole change of physical properties of the basement (Anderson et al., 1982; Becker et al., 1982). The data distinguish three geophysically distinct units which correspond to seismic Layers 2A, 2B, and 2C, respectively (see Fig. 1). Layer 2A is about 100 m thick and consists of a relatively permeable aquifer of rubbly pillow basalts and breccias with open, seawater-filled fractures. Electrical resistivity, density, and seismic velocities are very low within this zone. From 375 m to 875 m BSF all these properties show increasing gradients, whereas permeability and porosity drop significantly. Between 875 m and 925 m BSF, at about the depth of the stockwork, there is a pronounced change in all basement physical properties. Below 925 m a major increase in electrical resistivity, density, and seismic velocities is correlated with a strong decrease in porosity, permeability, and degree of fracturing. This zone is interpreted to be part of seismic Layer 2C.

This chapter deals with the chemical properties of the basement rocks recovered from Hole 504B. The following questions will be addressed:

1. What is the chemical composition and variation of the basement section drilled at this site?
2. Is there any difference between the upper volcanic and the lower dike section?
3. To what extent is the basement chemically affected by alteration processes?
4. Are there any systematic downhole variations of alteration-sensitive chemical parameters?
5. If so, how do they compare to the established downhole variations in alteration mineralogy and in physical properties of the basement?
6. What is the primary composition of the rocks?
7. What conclusions can be drawn about their mode of formation and ultimate origin?

MAJOR AND TRACE ELEMENT DATA

Analytical Methods

This study is based on chemical data obtained for 194 whole-rock samples, 37 of which are from the Leg 69 section, 68 from the Leg 70 section, and 89 from the Leg 83 section of the hole. Sample density is such that nearly every lithologic unit is represented by at least one sample. Care was taken always to select the "freshest possible," that is, the least altered material for analysis. The analytical methods used for the investigation of Leg 69 and 70 basalts and the results obtained were published by Hubberten et al. (1983).

Major element analyses of Leg 83 samples were performed using the following techniques:

1. Si, Ti, Al, Fe, Mn, Mg, Ca, Na, and P were measured by X-ray fluorescence analysis (XRF) on samples prepared as fused glass beads of lithium metaborate (rock to flux ratio 1:4), using a Philips PW 1400 computerized spectrometer for intensity measurements and Philips "alphas" program for concentration calculations.
2. Analyses for Fe^{2+} were conducted by manganometric titration.
3. A coulometric titration apparatus (Coulomat 700 Stroehlein) was used for the determination of CO_2 and S.
4. H_2O^+ was determined by Karl Fischer titration after thermal decomposition of the rock.
5. Atomic absorption spectroscopy (Perkin-Elmer AAS 5500) was used for control measurements of Mg and Na on selected samples.

For trace element determinations the following methods were applied:

1. Cr, Co, Ni, Cu, Zn, Ga, Sr, Y, and Zr were measured by XRF on pressed powder pellets using the Rh Compton peak of the X-ray tube for matrix corrections.
2. Flameless AAS was used to analyze K in selected samples.
3. Fluorine was measured by an ion-selective electrode following separation by pyrohydrolysis.
4. Analyses for the rare earth elements (REE) La, Ce, Pr, Nd, Sm, Eu, Gd, Tb, Dy, Ho, Er, Yb, and Lu were carried out by atomic emission spectroscopy (AES) using an inductively coupled plasma (ICP) for excitation. For this purpose the REE were quantitatively separated from rock dissolutions and concentrated by a chromatographic method. Sample preparation and analytical technique are described by Erzinger et al. (in press).

The precision of major and trace element determinations was tested by duplicate measurements of selected samples. Accuracy was always checked by carrying the reference rocks BIR-1, BM, BE-N, and BHVO-1 as "unknowns" through the whole procedure along with each set of Leg 83 samples. The chemical results obtained on these reference samples are given in Table 1 along with the respective analytical errors ($\pm 2s$) and the concentration values recommended in literature. This table also presents our chemical data for the three interlaboratory reference samples which were distributed among all laboratories that participated in the chemical investigation of Leg 83 rocks.

Results

Table 2 summarizes the major oxide compositions of the 89 samples from the Leg 83 portion of the hole. The values for Fe_2O_3^T (total iron calculated as Fe_2O_3) and for sulfur are listed separately. Sulfur concentrations above 0.2 wt. % were calculated as FeS_2 and listed among the major components. Also given are the mg-values, designated as mg_v , and calculated as atomic ratio of $\text{Mg}/(\text{Mg} + 0.85 \text{Fe})$, as well as the oxidation ratio Ox, which is the ratio (in wt. %) of Fe_2O_3 actually present to Fe_2O_3^T .

The trace element data are listed in Tables 2 and 3, respectively. Table 2 gives the concentrations for K, F, Cr, Co, Ni, Cu, Zn, Ga, Sr, Y, and Zr. The values for Rb and Nb in all samples were found to be below the detection limit of the method, that is, below 2 ppm. In Table 3, REE data are given for a few samples that were selected for analysis according to their major and trace element characteristics.

DISCUSSION

Before evaluating the chemical data obtained on Leg 83 samples the major results of the chemical investigations of the Legs 69 and 70 portion of the basement drilled at this site will be summarized. From the large number of analyses performed on least altered rock samples (Hubberten et al., 1983) and fresh basaltic glasses (Natland et al., 1983) the following main points emerged:

1. The remarkably uniform chemical composition of the volcanic layer.
2. The rather primitive, that is, unevolved, character of the majority of the basalts recovered.
3. The exceptional chemistry of two subordinate lava flows that occur at two thin intervals (i.e., Lithologic Units 5 and 36).

Except for basalts from Units 5 and 36, which differ markedly from all other basalts recovered, no significant chemical downhole variations could be established on the basis of whole-rock analyses. Most of the basalts are relatively MgO-rich (> 8 wt. %) and have mg_v -values of about 0.64 that clearly indicate that the respective magmas experienced only a limited degree of crystal fractionation prior to their eruption onto the seafloor. In contrast to other DSDP holes in the eastern Pacific (Leg 34, 54, 65, and 92), no ferrobasalts were cored at this site. According to their normative mineralogies the majority

Table 1A. Major element data for international reference rocks and Leg 83 samples selected for interlaboratory comparison.

| Major element oxides | BIR-1 | | | BM | | | Interlaboratory comparison, Hole 504B samples | | |
|---|------------|-------|---------------|------------|-------|-------------------|---|-------|--------|
| | This study | 2s | Gladney, 1983 | This study | 2s | Abbey, 1980, 1982 | 77-1, | 97-2, | 130-2, |
| | | | | | | | 44-53 | 74-89 | 44-58 |
| SiO ₂ | 47.89 | 0.30 | 47.94 ± 1.39 | 49.69 | 0.34 | 49.60 | 48.96 | 50.12 | 49.14 |
| TiO ₂ | 0.95 | 0.012 | 0.93 ± 0.05 | 1.11 | 0.02 | 1.14 | 0.92 | 0.955 | 0.75 |
| Al ₂ O ₃ | 15.76 | 0.10 | 14.76 ± 0.79 | 16.22 | 0.10 | 16.20 | 16.35 | 14.73 | 16.39 |
| Fe ₂ O ₃ ^T | 11.51 | 0.10 | 11.06 ± 0.56 | 9.66 | 0.10 | 9.68 | 9.84 | 10.56 | 9.01 |
| MnO | 0.18 | 0.004 | 0.17 ± 0.03 | 0.146 | 0.004 | 0.145 | 0.179 | 0.177 | 0.151 |
| MgO | 9.68 | 0.10 | 9.70 ± 0.99 | 7.49 | 0.08 | 7.46 | 8.27 | 8.39 | 9.12 |
| CaO | 13.32 | 0.10 | 13.02 ± 0.48 | 6.37 | 0.08 | 6.46 | 12.41 | 12.73 | 13.19 |
| Na ₂ O | 1.84 | 0.06 | 1.62 ± 0.09 | 4.87 | 0.10 | 4.64 | 2.45 | 2.00 | 1.73 |
| K ₂ O (XRF) | 0.033 | 0.002 | 0.017-0.040 | 0.183 | 0.004 | 0.203 | 0.032 | 0.017 | 0.015 |
| K ₂ O (AAS) | 0.037 | 0.002 | | 0.183 | 0.004 | | 0.024 | 0.009 | 0.008 |
| P ₂ O ₅ | 0.026 | 0.005 | 0.030-0.100 | 0.12 | 0.006 | 0.105 | 0.06 | 0.07 | 0.05 |

Table 1B. Trace element data for international reference rocks and Leg 83 samples selected for interlaboratory comparison.

| Trace elements | BE-N | | | BHVO-1 | | | Interlaboratory comparison, Hole 504B samples | | |
|----------------|------------|-----|---------------|------------|-----|-------------------|---|-------|--------|
| | This study | 2s | Gladney, 1983 | This study | 2s | Abbey, 1980, 1982 | 77-1, | 97-2, | 130-2, |
| | | | | | | | 44-53 | 74-89 | 44-58 |
| F | — | — | — | — | — | — | 83 | 66 | 63 |
| Cr | 373 | 7.4 | 360 | — | — | — | 301 | 259 | 373 |
| Co | 64 | 6.4 | 61 | — | — | — | 43 | 42 | 40 |
| Ni | 264 | 3.6 | 267 | — | — | — | 126 | 88 | 145 |
| Cu | 82 | 3.6 | 72 | — | — | — | 89 | 93 | 84 |
| Zn | 123 | 2.2 | 120 | — | — | — | 65 | 67 | 58 |
| Ga | 17 | 1.6 | 17 | — | — | — | 15 | 16 | 15 |
| Rb | — | — | — | 9 | 0.8 | 10 | <5 | <5 | <5 |
| Sr | — | — | — | 399 | 1.6 | 400 | 77 | 67 | 66 |
| Y | — | — | — | 27 | 1.2 | 27 | 25 | 27 | 21 |
| Zr | — | — | — | 176 | 1.6 | 180 | 61 | 63 | 51 |
| Nb | — | — | — | 18 | 0.8 | 19 | <5 | <5 | <5 |

Note: Dash indicates elements not determined.

of the basalts are to be classified as olivine tholeiites with only a few samples plotting close to the diopside-hypersthene join of the projected basalt tetrahedron.

For the major oxides the following ranges of variation (wt.%) and mean values (in parentheses) were found (Hubberten et al., 1983):

| | | | |
|--------------------------------|------------------|-------------------------------|------------------|
| SiO ₂ | 48.7-50.9 (49.9) | CaO | 11.2-13.5 (12.8) |
| TiO ₂ | 0.77-1.36 (0.93) | Na ₂ O | 1.93-2.73 (2.2) |
| Al ₂ O ₃ | 14.1-17.4 (15.3) | K ₂ O | 0.02-0.40 (0.04) |
| FeO ^T | 7.70-10.7 (9.2) | P ₂ O ₅ | 0.04-0.20 (0.07) |
| MgO | 6.67-9.39 (8.4) | | |

However, the majority of the samples show a much more restricted variation and cluster around the values given in brackets. When normalized to a dry weight basis these values closely correspond to the average glass composition as determined by Natland et al. (1983) on a total of 51 basalt glasses sampled throughout the pillow sequence down to about 800 m BSF (Table 4).

Whereas the whole-rock data do not establish significant chemical downhole variations, the glass compositions exhibit subtle but distinct chemical differences which could be used to define glass groups. Altogether 13 glass groups, that is, eruptive units, were distinguished within

the volcanic sequence; they are arranged in stratigraphic order. These units differ from each other in concentration of one or more major elements having almost identical compositions for all other elements. Their mg-values and TiO₂ contents, which are both very sensitive indicators of crystal fractionation processes, show virtually no differences. The mg-values range from 0.69 to 0.59, and most glass samples fall close to 0.64. The TiO₂ contents are less than 1.1 wt.% in most cases and cluster around 0.97 wt.%.

However, two glass groups are markedly set off from all other glass groups in being significantly enriched in TiO₂ (1.01 to 1.37 wt.%), Na₂O (2.36 to 2.53 wt.%), and P₂O₅ (0.09 to 0.16 wt.%) at similar MgO concentrations. These groups represent Lithologic Units 5 and 36, which from whole-rock analyses were also recognized as "anomalous" basalt types high in Ti, Na, and P (Hubberten et al., 1983). Excluding the samples from Units 5 and 36 the average composition of the fresh basaltic glasses is very similar to the respective average of the least altered basalts. The means and standard deviations of 51 glass samples and of 58 least altered basalts from the Leg 69 and 70 sections of the hole are given in Table 4. On a 99.5% confidence level these two means are indistinguishable.

The chemical differences between basalts from Units 5 and 36 and all other basalts recovered from the volcanic layer are even more pronounced when their trace element characteristics are examined (cf. Marsh et al., 1983). Whereas the majority of the basalts are strongly depleted in hygromagmaphile elements, basalts from Units 5 and 36 have distinctly higher concentrations in incompatible elements. These differences are especially well documented by the respective REE distribution patterns. Figure 2 shows the chondrite-normalized REE distribution curves for Units 5 and 36 basalts and gives the range of variation of the REE patterns of all other basalts. In contrast to the majority of the basalts, which are strongly depleted in light REE (La/Sm enrichment factor about 0.4) basalts from Units 5 and 36 exhibit almost chondritic or even light-REE-enriched patterns which are normally regarded as typical for "plume"-derived basaltic melts.

The pronounced mineralogical alteration which affected the basalts of the pillow section and which distinguished two different alteration types (see introduction) is not reflected in systematic concentration changes in most of the elements analyzed. Only potassium, sulfur, and the iron oxidation ratio were found to be suitable discriminants between the upper oxidative and the lower non-oxidative alteration zone. The values published by Hubberten et al. (1983) are incorporated into Figure 3, which is a chemical downhole alteration plot of the basaltic basement cored at Site 504. This figure is based on all the 194 least altered whole-rock samples. Among the components determined, H_2O^+ , CO_2 , K, S, and Mn as well as the iron oxidation ratio (Ox) proved to be sensitive indicators of the alteration processes which affected the basement at this site. A close scrutiny of Figure 3 reveals that all six alteration parameters display pronounced and systematic changes with depth.

H_2O^+ is relatively low and uniform in the upper portion of the basement down to 836 m BSF, with concentrations mostly falling close to 1.0 wt.%. Below this depth it increases abruptly and reaches a maximum (4.35 wt.%) in the interval between 910 and 1059 m BSF. Further downward the H_2O^+ contents drop again and cluster around 1.5 wt.% in the lowest part of the hole. CO_2 shows a different behavior. In general, a systematic downhole decrease from values slightly above 0.1 wt.% at the sediment/basement interface to values of about 0.05 wt.% at the bottom of the hole can be established. However, over this general trend are superimposed some higher and more scattered values, especially in the intervals between 274 and 530 m BSF and 910 to 1059 m BSF; these are probably due to the presence of minor calcite-bearing veinlets in the respective samples.

Potassium also exhibits a general concentration decrease from top to bottom of the cored basement section. It is strongly enriched and scatters considerably in the uppermost part of the pillow section, down about 530 m BSF. Within this interval the K_2O concentrations range from 0.02 to 0.40 wt.% and average at 0.20 wt.%. Below 560 m BSF, K_2O decreases abruptly to values of less than 0.04 wt.% in most samples. From the very precise potassium determinations obtained by flameless AAS

a systematic downhole decrease of K from 200 ppm to less than 100 ppm can be established for the Leg 83 section of the hole (see Fig. 4).

Whole-rock sulfur contents vary between 0.02 and 1.95 wt.%. They are lowest in the uppermost K_2O enriched zone of the basement where they average 0.03 wt.%. The highest sulfur concentrations occur in the depth interval between 910 and 1059 m BSF. Above and below this zone sulfur contents are mostly between 0.05 and 0.10 wt.%.

The iron oxidation ratio changes systematically with depth, showing distinct zones which clearly reflect significant differences in redox conditions. Basalts recovered from the uppermost part of the basement are most strongly oxidized, having Ox values of 0.40 on an average. The lowest Ox values occur in the depth interval between 910 and 1059 m BSF. Basaltic rocks from this basement portion have oxidation ratios of close to 0.20.

Manganese contents of the basalts are, in general, rather uniform and range between 0.16 and 0.19 wt.% MnO in most samples. However, within the depth interval from 910 to 1059 m BSF manganese is invariably enriched and increases up to 0.39 wt.% MnO. This zone is also characterized by an anomalous concentration distribution of both Cu and Zn, as is to be seen from Figure 4, which shows the downhole variation of some selected trace elements for the Leg 83 portion of the hole. Whereas the Cu contents of the basalts normally range from 70 to 100 ppm, in the interval from 910 to 1059 m BSF they display a considerable scatter, being strongly enriched in some samples (up to 567 ppm) and obviously depleted in others (down to 10 ppm).

Zn also exhibits an anomalous concentration distribution within this depth interval, although there is not obvious correlation between the two elements. Zn concentrations are rather uniform in basalts above 910 m and below 1059 m BSF, varying mostly between 60 and 80 ppm. In the interval from 910 to 1059 m BSF, Zn contents scatter considerably and increase up to 1630 ppm. However, a conspicuous Zn depletion analogous to the Cu depletion is not observed.

In contrast to these elements neither Ni nor Cr display any systematic changes with depth which could be related to secondary redistribution processes. Their concentrations vary quite irregularly, obviously reflecting primary compositional differences among the basaltic lithologies recovered.

The chemical data presented in Figures 3 and 4 distinguish five or six distinct alteration zones which are more or less sharply set off from each other. These zones closely reflect the downhole variations in alteration mineralogy outlined in the introduction. Accordingly, two significantly different types of chemical alteration are to be observed within the volcanic layer. Basalts from the uppermost portion of the pillow sequence (down to about 530 m BSF) are characterized by a marked potassium enrichment, the highest iron oxidation ratios and the lowest sulfur contents. This alteration undoubtedly has been caused by low-temperature "seawater-weathering" or halmyrolysis, which resulted in potassium uptake and iron oxidation as well as sulfur loss through sulfide

Table 2. Major oxide and trace element composition of least altered basement rocks from samples in the Leg 83 section of Hole 504B.

| Core-Section (interval in cm) | 71-1, 6-8 | 72-1, 40-42 | 72-1, 74-76 | 72-1, 96-98 | 72-3, 123-125 | 72-4, 60-62 | 73-1, 47-49 | 73-1, 124-126 | 73-2, 58-60 | 74-1, 90-93 | 75-1, 91-93 | 76-1, 51-53 | 77-1, 44-53 | 77-2, 80-82 | 77-3, 30-33 | |
|---|--------------|----------------|----------------|----------------|------------------|----------------|----------------|------------------|----------------|----------------|----------------|----------------|----------------|----------------|----------------|--|
| Sub-bottom depth (m) | 836.07 | 843.91 | 844.25 | 844.47 | 847.74 | 848.61 | 852.98 | 853.75 | 854.59 | 862.42 | 871.42 | 880.02 | 888.99 | 890.81 | 891.82 | |
| Lithologic unit | 47 | 47 | 48 | 48 | 49 | 50 | 50 | 50 | 50 | 52 | 52 | 53 | 54 | 55 | 55 | |
| Major element oxides | | | | | | | | | | | | | | | | |
| SiO ₂ | 49.1 | 48.2 | 49.3 | 49.4 | 48.4 | 48.4 | 49.0 | 49.1 | 49.3 | 48.7 | 48.2 | 48.3 | 48.8 | 50.3 | 49.1 | |
| TiO ₂ | 0.83 | 0.90 | 0.85 | 0.84 | 0.90 | 0.93 | 0.83 | 0.81 | 0.82 | 0.92 | 0.90 | 0.90 | 0.92 | 1.04 | 1.02 | |
| Al ₂ O ₃ | 16.5 | 16.5 | 16.3 | 16.3 | 16.3 | 16.5 | 15.7 | 15.8 | 16.3 | 16.6 | 16.0 | 16.0 | 16.4 | 14.3 | 14.9 | |
| Fe ₂ O ₃ | 3.89 | 4.03 | 3.34 | 3.51 | 3.42 | 2.85 | 2.43 | 2.76 | 2.88 | 3.81 | 4.11 | 3.29 | 3.08 | 2.55 | 3.22 | |
| FeO | 5.05 | 4.82 | 5.50 | 5.28 | 5.52 | 6.10 | 6.36 | 5.78 | 5.86 | 5.09 | 5.04 | 5.93 | 6.08 | 6.80 | 7.00 | |
| MnO | 0.19 | 0.16 | 0.16 | 0.19 | 0.15 | 0.16 | 0.16 | 0.17 | 0.17 | 0.19 | 0.17 | 0.18 | 0.18 | 0.19 | 0.18 | |
| MgO | 9.04 | 8.40 | 8.77 | 8.48 | 9.06 | 8.91 | 9.13 | 9.04 | 8.89 | 7.98 | 8.83 | 8.91 | 8.28 | 8.43 | 8.38 | |
| CaO | 12.1 | 12.4 | 12.7 | 12.8 | 12.0 | 12.0 | 12.6 | 13.0 | 12.6 | 12.7 | 12.4 | 12.3 | 12.4 | 11.6 | 12.2 | |
| Na ₂ O | 1.77 | 2.06 | 1.93 | 1.95 | 2.13 | 2.13 | 1.94 | 1.86 | 1.92 | 2.20 | 2.01 | 1.97 | 2.45 | 2.41 | 2.21 | |
| K ₂ O | 0.03 | 0.08 | 0.02 | 0.02 | 0.02 | 0.03 | 0.04 | 0.03 | 0.02 | 0.02 | 0.02 | 0.02 | 0.03 | 0.02 | 0.04 | |
| P ₂ O ₅ | 0.06 | 0.06 | 0.06 | 0.06 | 0.06 | 0.06 | 0.06 | 0.06 | 0.06 | 0.06 | 0.06 | 0.06 | 0.06 | 0.08 | 0.07 | |
| H ₂ O ⁺ | 1.68 | 2.56 | 1.43 | 1.49 | 2.21 | 2.03 | 1.38 | 1.49 | 1.34 | 1.89 | 2.36 | 2.21 | 1.60 | 1.87 | 1.84 | |
| CO ₂ | 0.18 | 0.26 | 0.11 | 0.09 | 0.13 | 0.14 | 0.12 | 0.14 | 0.10 | 0.12 | 0.13 | 0.09 | 0.13 | 0.06 | 0.06 | |
| FeS ₂ | — | — | — | — | — | — | — | — | — | — | — | — | — | — | — | |
| Σ | 100.42 | 100.43 | 100.47 | 100.41 | 100.30 | 100.24 | 99.75 | 100.04 | 100.26 | 100.28 | 100.23 | 100.16 | 100.41 | 99.65 | 100.22 | |
| Fe ₂ O ₃ ^T | 9.50 | 9.39 | 9.45 | 9.38 | 9.55 | 9.63 | 9.50 | 9.18 | 9.39 | 9.46 | 9.71 | 9.88 | 9.83 | 10.1 | 11.0 | |
| S | 0.02 | 0.04 | 0.04 | 0.06 | 0.04 | 0.05 | 0.09 | 0.08 | 0.07 | 0.06 | 0.03 | 0.08 | 0.07 | 0.10 | 0.06 | |
| Ox | 0.410 | 0.429 | 0.353 | 0.374 | 0.358 | 0.296 | 0.256 | 0.301 | 0.307 | 0.403 | 0.423 | 0.333 | 0.313 | 0.252 | 0.293 | |
| mg _v | 0.689 | 0.676 | 0.684 | 0.678 | 0.689 | 0.683 | 0.691 | 0.697 | 0.688 | 0.663 | 0.679 | 0.678 | 0.663 | 0.661 | 0.640 | |
| Trace elements | | | | | | | | | | | | | | | | |
| K | 210 | n.d. | n.d. | 138 | n.d. | n.d. | n.d. | 142 | n.d. | n.d. | n.d. | 127 | 201 | 147 | 236 | |
| F | 71 | n.d. | n.d. | n.d. | 77 | n.d. | 63 | n.d. | n.d. | n.d. | n.d. | n.d. | 83 | 97 | n.d. | |
| Cr | 348 | 356 | 362 | 367 | 354 | 364 | 354 | 361 | 332 | 348 | 346 | 352 | 301 | 202 | 235 | |
| Co | 40 | 40 | 47 | 42 | 41 | 44 | 44 | 39 | 43 | 43 | 44 | 43 | 43 | 46 | 44 | |
| Ni | 130 | 130 | 137 | 140 | 126 | 126 | 138 | 142 | 145 | 127 | 128 | 151 | 126 | 78 | 86 | |
| Cu | 79 | 69 | 81 | 80 | 78 | 89 | 79 | 78 | 77 | 87 | 85 | 85 | 89 | 75 | 85 | |
| Zn | 71 | 61 | 68 | 65 | 64 | 69 | 67 | 63 | 66 | 66 | 66 | 62 | 65 | 92 | 87 | |
| Ga | 15 | 16 | 15 | 15 | 15 | 15 | 15 | 15 | 15 | 15 | 15 | 14 | 15 | 17 | 16 | |
| Sr | 54 | 70 | 68 | 69 | 69 | 73 | 67 | 63 | 67 | 80 | 72 | 74 | 77 | 60 | 58 | |
| Y | 24 | 24 | 24 | 23 | 24 | 25 | 23 | 23 | 22 | 25 | 24 | 24 | 25 | 29 | 29 | |
| Zr | 52 | 60 | 55 | 55 | 60 | 60 | 55 | 54 | 53 | 62 | 60 | 60 | 61 | 65 | 64 | |

Table 2. (Continued).

| Core-Section (interval in cm) | 92-2, 2-6 | 93-1, 69-77 | 93-2, 27-29 | 93-3, 21-25 | 93-3, 77-79 | 94-1, 12-16 | 95-1, 140-143 | 96-1, 102-105 | 97-1, 6-8 | 97-2, 74-89 | 98-1, 42-45 | 99-1, 103-105 | 100-3, 61-65 | 101-1, 110-114 |
|---|--------------|----------------|----------------|----------------|----------------|----------------|------------------|------------------|--------------|----------------|----------------|------------------|-----------------|-------------------|
| Sub-bottom depth (m) | 1014.04 | 1022.23 | 1023.28 | 1024.73 | 1025.28 | 1030.64 | 1040.92 | 1049.53 | 1057.57 | 1059.82 | 1062.44 | 1072.54 | 1084.13 | 1090.62 |
| Lithologic unit | 78 | 81 | 81 | 83 | 83 | 84 | 88 | 90 | 91 | 91 | 93 | 94 | 99 | 102 |
| Major element oxides | | | | | | | | | | | | | | |
| SiO ₂ | 49.8 | 50.3 | 50.9 | 47.2 | 47.3 | 49.8 | 51.1 | 48.7 | 48.0 | 50.1 | 49.5 | 49.3 | 47.9 | 49.2 |
| TiO ₂ | 1.05 | 1.28 | 0.83 | 1.50 | 1.51 | 0.92 | 0.98 | 0.65 | 0.77 | 0.96 | 1.13 | 0.91 | 0.78 | 0.86 |
| Al ₂ O ₃ | 14.2 | 12.9 | 14.6 | 15.6 | 15.1 | 15.7 | 14.0 | 16.5 | 14.6 | 14.7 | 15.1 | 14.3 | 16.1 | 15.1 |
| Fe ₂ O ₃ | 2.39 | 2.23 | 1.62 | 2.27 | 2.13 | 2.57 | 2.01 | 2.19 | 2.49 | 2.92 | 2.56 | 2.57 | 2.09 | 2.17 |
| FeO | 6.65 | 8.84 | 7.43 | 7.50 | 7.89 | 6.66 | 7.73 | 5.87 | 6.10 | 6.91 | 7.42 | 7.14 | 6.91 | 7.01 |
| MnO | 0.23 | 0.30 | 0.23 | 0.21 | 0.22 | 0.18 | 0.21 | 0.15 | 0.31 | 0.18 | 0.22 | 0.22 | 0.19 | 0.19 |
| MgO | 8.42 | 8.09 | 8.20 | 8.50 | 8.83 | 8.33 | 7.93 | 9.46 | 9.28 | 8.38 | 7.69 | 8.63 | 8.81 | 8.77 |
| CaO | 12.0 | 10.8 | 11.2 | 11.5 | 10.8 | 12.8 | 11.8 | 13.3 | 12.2 | 12.7 | 12.2 | 12.4 | 13.3 | 12.8 |
| Na ₂ O | 1.80 | 2.13 | 1.96 | 2.35 | 2.40 | 1.88 | 2.08 | 1.59 | 1.72 | 2.00 | 1.98 | 2.24 | 1.79 | 2.05 |
| K ₂ O | 0.02 | 0.02 | 0.02 | 0.02 | 0.03 | 0.02 | 0.02 | 0.02 | 0.03 | 0.02 | 0.02 | 0.02 | 0.02 | 0.02 |
| P ₂ O ₅ | 0.08 | 0.10 | 0.07 | 0.18 | 0.18 | 0.07 | 0.07 | 0.05 | 0.06 | 0.07 | 0.09 | 0.06 | 0.05 | 0.06 |
| H ₂ O ⁺ | 2.23 | 2.85 | 3.17 | 3.33 | 3.77 | 1.44 | 2.28 | 1.73 | 3.32 | 0.88 | 2.15 | 2.57 | 2.24 | 2.02 |
| CO ₂ | 0.08 | 0.09 | 0.08 | 0.08 | 0.12 | 0.07 | 0.08 | 0.08 | 0.20 | 0.11 | 0.08 | 0.06 | 0.06 | 0.07 |
| FeS ₂ | 1.10 | 0.37 | — | — | — | — | — | — | 1.10 | — | — | — | — | — |
| Σ | 100.05 | 100.30 | 100.31 | 100.24 | 100.28 | 100.44 | 100.29 | 100.29 | 100.18 | 99.94 | 100.14 | 100.42 | 100.24 | 100.32 |
| Fe ₂ O ₃ ^T | 10.5 | 12.3 | 9.87 | 10.6 | 10.9 | 9.97 | 10.6 | 8.71 | 10.0 | 10.6 | 10.8 | 10.5 | 9.77 | 9.96 |
| S | 0.59 | 0.20 | 0.04 | 0.01 | 0.02 | 0.07 | 0.02 | 0.05 | 0.59 | 0.10 | 0.05 | 0.04 | 0.02 | 0.10 |
| Ox | 0.228 | 0.181 | 0.164 | 0.214 | 0.195 | 0.258 | 0.190 | 0.251 | 0.249 | 0.275 | 0.237 | 0.245 | 0.214 | 0.218 |
| mg _v | 0.651 | 0.605 | 0.659 | 0.651 | 0.654 | 0.661 | 0.636 | 0.717 | 0.684 | 0.648 | 0.624 | 0.657 | 0.678 | 0.672 |
| Trace elements | | | | | | | | | | | | | | |
| K | 100 | n.d. | n.d. | n.d. | n.d. | n.d. | 103 | 110 | 133 | 75 | 91 | n.d. | n.d. | n.d. |
| F | 71 | 102 | n.d. | 150 | n.d. | n.d. | n.d. | n.d. | n.d. | 66 | n.d. | n.d. | n.d. | n.d. |
| Cr | 310 | 108 | 323 | 260 | 271 | 282 | 212 | 336 | 431 | 259 | 257 | 224 | 340 | 316 |
| Co | 45 | 51 | 36 | 43 | 47 | 42 | 49 | 41 | 41 | 42 | 39 | 44 | 43 | 43 |
| Ni | 86 | 62 | 89 | 134 | 133 | 101 | 79 | 156 | 128 | 88 | 96 | 86 | 120 | 94 |
| Cu | 259 | 417 | 189 | 27 | 12 | 76 | 111 | 87 | 92 | 92 | 161 | 72 | 65 | 66 |
| Zn | 88 | 104 | 89 | 81 | 89 | 66 | 71 | 52 | 101 | 67 | 80 | 74 | 71 | 82 |
| Ga | 15 | 15 | 14 | 17 | 15 | 17 | 15 | 14 | 14 | 16 | 15 | 16 | 16 | 15 |
| Sr | 60 | 49 | 56 | 84 | 85 | 59 | 54 | 53 | 42 | 67 | 52 | 51 | 52 | 57 |
| Y | 30 | 35 | 23 | 35 | 35 | 25 | 27 | 20 | 23 | 27 | 31 | 25 | 21 | 25 |
| Zr | 75 | 83 | 58 | 139 | 142 | 57 | 62 | 43 | 48 | 63 | 73 | 55 | 49 | 52 |

Table 2. (Continued).

| 78-1, 126-128 | 79-1, 58-60 | 79-3, 79-81 | 80-1, 38-41 | 80-4, 33-36 | 81-1, 99-101 | 82-1, 81-84 | 82-3, 54-62 | 83-1, 70-73 | 84-1, 85-87 | 85-1, 37-39 | 85-2, 127-131 | 87-2, 37-40 | 88-1, 111-115 | 89-2, 95-98 | 90-4, 146-149 | 91-1, 78-80 |
|------------------|----------------|----------------|----------------|----------------|-----------------|----------------|----------------|----------------|----------------|----------------|------------------|----------------|------------------|----------------|------------------|----------------|
| 898.77 | 905.09 | 908.30 | 910.40 | 914.85 | 920.50 | 929.33 | 932.08 | 938.22 | 947.36 | 955.88 | 958.29 | 968.89 | 977.63 | 987.97 | 1000.48 | 1004.29 |
| 57 | 59 | 59 | 60 | 60 | 60 | 60 | 60 | 60 | 60 | 60 | 61 | 66 | 70 | 71 | 72 | 75 |
| 48.1 | 48.6 | 47.9 | 46.0 | 47.4 | 49.2 | 49.5 | 49.1 | 46.7 | 48.8 | 50.4 | 48.6 | 48.5 | 49.3 | 48.0 | 50.7 | 48.5 |
| 0.90 | 0.91 | 0.91 | 0.86 | 0.80 | 0.87 | 0.90 | 0.87 | 0.56 | 0.84 | 0.92 | 0.86 | 1.01 | 1.05 | 0.94 | 0.85 | 0.72 |
| 16.1 | 16.3 | 16.6 | 17.1 | 17.0 | 15.4 | 15.3 | 15.5 | 15.6 | 14.9 | 14.5 | 14.9 | 15.3 | 15.1 | 14.1 | 15.0 | 15.6 |
| 2.60 | 2.43 | 3.03 | 1.62 | 2.00 | 1.89 | 2.38 | 1.37 | 1.46 | 1.92 | 1.62 | 2.03 | 1.92 | 1.76 | 2.13 | 1.85 | 1.67 |
| 6.33 | 5.97 | 5.92 | 5.11 | 5.62 | 6.97 | 7.04 | 6.76 | 5.96 | 6.39 | 7.29 | 7.13 | 7.24 | 7.20 | 8.16 | 6.60 | 6.85 |
| 0.18 | 0.16 | 0.15 | 0.33 | 0.27 | 0.23 | 0.22 | 0.23 | 0.39 | 0.28 | 0.37 | 0.25 | 0.30 | 0.23 | 0.26 | 0.22 | 0.27 |
| 9.15 | 8.38 | 8.23 | 7.95 | 9.13 | 8.74 | 8.54 | 8.59 | 9.72 | 9.33 | 8.35 | 9.05 | 8.66 | 8.67 | 8.61 | 8.29 | 9.25 |
| 12.2 | 13.3 | 12.8 | 11.6 | 12.2 | 13.1 | 12.9 | 12.5 | 11.2 | 11.9 | 11.0 | 11.6 | 11.9 | 12.3 | 11.2 | 11.1 | 12.8 |
| 2.25 | 2.15 | 2.24 | 2.32 | 1.99 | 1.79 | 1.80 | 1.68 | 1.90 | 1.72 | 1.83 | 2.41 | 2.07 | 2.04 | 2.22 | 1.88 | 1.76 |
| 0.03 | 0.02 | 0.02 | 0.02 | 0.02 | 0.02 | 0.02 | 0.02 | 0.02 | 0.02 | 0.02 | 0.02 | 0.03 | 0.04 | 0.02 | 0.02 | 0.02 |
| 0.06 | 0.06 | 0.06 | 0.05 | 0.05 | 0.06 | 0.07 | 0.06 | 0.04 | 0.07 | 0.07 | 0.06 | 0.10 | 0.11 | 0.07 | 0.07 | 0.05 |
| 2.46 | 1.88 | 2.21 | 2.92 | 2.82 | 1.77 | 1.45 | 2.12 | 4.04 | 2.55 | 3.07 | 3.31 | 3.30 | 2.62 | 4.35 | 3.41 | 2.21 |
| 0.12 | 0.08 | 0.09 | 0.18 | 0.17 | 0.08 | 0.12 | 0.11 | 0.55 | 0.10 | 0.06 | 0.12 | 0.07 | 0.07 | 0.24 | 0.34 | 0.07 |
| — | — | — | 3.65 | 0.41 | 0.37 | — | 1.14 | 1.93 | 1.18 | 0.73 | — | — | — | — | — | 0.58 |
| 100.48 | 100.24 | 100.16 | 99.71 | 99.88 | 100.49 | 100.24 | 100.05 | 100.07 | 100.00 | 100.23 | 100.34 | 100.40 | 100.49 | 100.30 | 100.33 | 100.35 |
| 9.63 | 9.06 | 9.61 | 9.73 | 8.51 | 9.87 | 10.2 | 9.64 | 9.37 | 9.80 | 10.2 | 9.95 | 9.96 | 9.76 | 11.2 | 9.18 | 9.67 |
| 0.06 | 0.10 | 0.10 | 1.95 | 0.22 | 0.20 | 0.13 | 0.61 | 1.03 | 0.63 | 0.39 | 0.09 | 0.05 | 0.04 | 0.09 | 0.06 | 0.31 |
| 0.270 | 0.268 | 0.315 | 0.166 | 0.235 | 0.191 | 0.233 | 0.142 | 0.156 | 0.196 | 0.159 | 0.204 | 0.193 | 0.180 | 0.190 | 0.202 | 0.173 |
| 0.689 | 0.683 | 0.666 | 0.656 | 0.714 | 0.674 | 0.661 | 0.675 | 0.707 | 0.689 | 0.656 | 0.680 | 0.670 | 0.674 | 0.642 | 0.678 | 0.690 |
| n.d. | n.d. | n.d. | 107 | 92 | n.d. | n.d. | n.d. | 142 | 69 | 71 | n.d. | n.d. | 202 | 120 | n.d. | n.d. |
| 77 | 77 | 65 | 66 | 61 | 67 | n.d. | n.d. | 46 | n.d. | 76 | 67 | 96 | 104 | n.d. | n.d. | 57 |
| 327 | 327 | 341 | 424 | 379 | 374 | 356 | 345 | 365 | 360 | 227 | 379 | 307 | 290 | 186 | 287 | 385 |
| 48 | 39 | 41 | 45 | 38 | 42 | 41 | 42 | 35 | 41 | 36 | 44 | 40 | 39 | 41 | 35 | 39 |
| 136 | 128 | 136 | 148 | 160 | 120 | 110 | 116 | 170 | 123 | 83 | 105 | 103 | 96 | 93 | 96 | 125 |
| 102 | 86 | 113 | 50 | 118 | 80 | 76 | 71 | 15 | 65 | 96 | 76 | 332 | 215 | 567 | 276 | 83 |
| 68 | 61 | 59 | 1630 | 155 | 82 | 77 | 89 | 177 | 102 | 140 | 104 | 120 | 91 | 100 | 97 | 96 |
| 16 | 14 | 14 | 15 | 14 | 15 | 15 | 14 | 14 | 14 | 15 | 15 | 14 | 15 | 13 | 14 | 15 |
| 72 | 76 | 78 | 61 | 59 | 54 | 56 | 52 | 45 | 50 | 51 | 68 | 78 | 79 | 76 | 64 | 44 |
| 24 | 25 | 24 | 24 | 22 | 25 | 25 | 25 | 17 | 24 | 27 | 24 | 25 | 26 | 26 | 23 | 21 |
| 60 | 62 | 61 | 56 | 53 | 57 | 58 | 58 | 38 | 56 | 61 | 58 | 74 | 79 | 56 | 60 | 46 |

Table 2. (Continued).

| 101-2, 116-119 | 102-1, 47-49 | 103-1, 92-95 | 104-2, 2-6 | 105-1, 5-8 | 106-1, 47-49 | 107-1, 124-128 | 108-1, 20-23 | 109-1, 77-80 | 111-1, 94-97 | 112-1, 43-46 | 113-1, 37-41 | 116-1, 50-52 | 117-1, 32-35 | 117-1, 126-130 | 121-1, 46-49 |
|-------------------|-----------------|-----------------|---------------|---------------|-----------------|-------------------|-----------------|-----------------|-----------------|-----------------|-----------------|-----------------|-----------------|-------------------|-----------------|
| 1092.17 | 1098.98 | 1108.44 | 1118.04 | 1125.57 | 1134.98 | 1144.76 | 1152.72 | 1154.28 | 1162.46 | 1166.45 | 1171.39 | 1185.51 | 1189.84 | 1190.78 | 1207.98 |
| 103 | 103 | 105 | 106 | 107 | 109 | 111 | 111 | 112 | 113 | 115 | 115 | 117 | 118 | 118 | 120 |
| 49.3 | 48.9 | 49.0 | 49.8 | 49.3 | 48.4 | 50.3 | 50.5 | 49.9 | 45.7 | 49.4 | 49.2 | 48.2 | 49.3 | 49.8 | 50.5 |
| 0.86 | 0.81 | 0.85 | 0.91 | 1.03 | 0.83 | 0.86 | 0.87 | 0.91 | 0.92 | 0.84 | 0.74 | 0.94 | 0.92 | 0.91 | 0.98 |
| 16.0 | 15.5 | 15.4 | 15.9 | 14.2 | 15.2 | 14.9 | 14.7 | 15.5 | 17.6 | 15.0 | 15.9 | 14.8 | 15.3 | 15.7 | 14.9 |
| 2.33 | 2.67 | 1.91 | 2.50 | 2.63 | 2.41 | 2.73 | 2.67 | 2.76 | 3.98 | 2.69 | 2.69 | 2.79 | 2.78 | 2.65 | 2.86 |
| 6.45 | 6.16 | 7.15 | 6.62 | 8.52 | 7.10 | 6.54 | 6.78 | 6.79 | 5.69 | 6.94 | 6.16 | 7.21 | 6.77 | 6.71 | 7.24 |
| 0.18 | 0.16 | 0.18 | 0.17 | 0.22 | 0.19 | 0.17 | 0.17 | 0.17 | 0.14 | 0.18 | 0.16 | 0.18 | 0.18 | 0.17 | 0.18 |
| 7.99 | 8.84 | 8.63 | 8.29 | 8.06 | 8.87 | 8.71 | 8.80 | 8.06 | 8.95 | 8.65 | 9.02 | 8.70 | 8.49 | 8.21 | 8.02 |
| 12.5 | 12.8 | 13.2 | 12.9 | 11.8 | 13.1 | 13.0 | 12.8 | 12.8 | 12.5 | 13.1 | 13.1 | 12.3 | 13.0 | 12.9 | 12.7 |
| 2.23 | 2.17 | 2.06 | 1.91 | 2.43 | 1.90 | 1.88 | 1.93 | 1.84 | 1.79 | 1.73 | 1.74 | 2.38 | 2.05 | 1.79 | 1.80 |
| 0.02 | 0.02 | 0.02 | 0.02 | 0.02 | 0.02 | 0.02 | 0.02 | 0.02 | 0.03 | 0.02 | 0.02 | 0.02 | 0.02 | 0.02 | 0.02 |
| 0.06 | 0.06 | 0.06 | 0.07 | 0.07 | 0.05 | 0.07 | 0.07 | 0.07 | 0.06 | 0.06 | 0.05 | 0.07 | 0.07 | 0.06 | 0.07 |
| 2.44 | 2.25 | 1.93 | 1.17 | 2.12 | 2.20 | 1.02 | 0.84 | 1.41 | 3.01 | 0.99 | 1.54 | 2.59 | 1.40 | 1.07 | 1.16 |
| 0.06 | 0.08 | 0.06 | 0.07 | 0.06 | 0.06 | 0.07 | 0.07 | 0.06 | 0.11 | 0.07 | 0.07 | 0.09 | 0.06 | 0.07 | 0.05 |
| 100.42 | 100.42 | 100.45 | 100.33 | 100.46 | 100.33 | 100.27 | 100.22 | 100.29 | 100.48 | 99.67 | 100.39 | 100.27 | 100.24 | 100.06 | 100.48 |
| 9.50 | 9.51 | 9.85 | 9.85 | 12.1 | 10.3 | 10.0 | 10.2 | 10.3 | 10.3 | 10.4 | 9.53 | 10.8 | 10.3 | 10.1 | 10.9 |
| 0.05 | 0.12 | 0.04 | 0.07 | 0.05 | 0.04 | 0.10 | 0.09 | 0.07 | 0.05 | 0.08 | 0.07 | 0.01 | 0.10 | 0.10 | 0.11 |
| 0.245 | 0.281 | 0.194 | 0.254 | 0.217 | 0.234 | 0.273 | 0.262 | 0.268 | 0.386 | 0.259 | 0.282 | 0.258 | 0.270 | 0.262 | 0.262 |
| 0.662 | 0.684 | 0.671 | 0.662 | 0.608 | 0.667 | 0.670 | 0.668 | 0.646 | 0.669 | 0.660 | 0.688 | 0.653 | 0.658 | 0.655 | 0.632 |
| n.d. | 108 | n.d. | n.d. | 101 | n.d. | n.d. | n.d. | 80 | n.d. | n.d. | n.d. | 100 | n.d. | n.d. | n.d. |
| 50 | n.d. | n.d. | 64 | 80 | n.d. | n.d. | n.d. | n.d. | 97 | n.d. | n.d. | 56 | 72 | n.d. | n.d. |
| 259 | 391 | 316 | 347 | 128 | 370 | 309 | 287 | 244 | 519 | 352 | 346 | 324 | 399 | 303 | 229 |
| 38 | 41 | 43 | 41 | 52 | 40 | 42 | 43 | 36 | 52 | 45 | 39 | 47 | 45 | 39 | 45 |
| 89 | 106 | 93 | 108 | 62 | 102 | 94 | 89 | 83 | 288 | 99 | 124 | 96 | 102 | 103 | 81 |
| 43 | 76 | 94 | 80 | 84 | 71 | 87 | 86 | 79 | 81 | 94 | 84 | 33 | 76 | 77 | 77 |
| 70 | 70 | 63 | 66 | 80 | 57 | 68 | 67 | 58 | 68 | 76 | 71 | 46 | 71 | 67 | 76 |
| 15 | 15 | 15 | 16 | 16 | 15 | 16 | 16 | 17 | 17 | 16 | 15 | 15 | 17 | 16 | 16 |
| 63 | 61 | 64 | 65 | 55 | 54 | 60 | 62 | 54 | 92 | 55 | 55 | 53 | 54 | 53 | 50 |
| 23 | 23 | 24 | 26 | 29 | 25 | 24 | 25 | 26 | 24 | 24 | 21 | 27 | 26 | 26 | 28 |
| 54 | 50 | 55 | 59 | 61 | 51 | 56 | 56 | 58 | 68 | 52 | 47 | 55 | 57 | 57 | 61 |

Table 2. (Continued).

| Core-Section (interval in cm) | 122-1, 98-100 | 123-1, 60-64 | 124-1, 81-84 | 125-1, 25-28 | 125-1, 76-79 | 127-1, 25-28 | 127-1, 101-105 | 128-1, 69-72 | 128-1, 126-130 | 129-1, 3-7 | 129-2, 58-62 | 129-3, 94-96 | 129-3, 112-116 | 130-1, 36-40 |
|---|------------------|-----------------|-----------------|-----------------|-----------------|-----------------|-------------------|-----------------|-------------------|---------------|-----------------|-----------------|-------------------|-----------------|
| Sub-bottom depth (m) | 1214.49 | 1223.12 | 1232.33 | 1240.77 | 1241.28 | 1253.77 | 1254.53 | 1261.71 | 1262.28 | 1270.05 | 1272.10 | 1273.95 | 1274.14 | 1279.38 |
| Lithologic unit | 122 | 124 | 126 | 126 | 126 | 131 | 131 | 132 | 133 | 133 | 133 | 134 | 135 | 135 |
| Major element oxides | | | | | | | | | | | | | | |
| SiO ₂ | 48.9 | 49.0 | 49.2 | 49.0 | 49.7 | 49.2 | 49.0 | 49.0 | 48.7 | 48.7 | 48.6 | 49.7 | 49.2 | 48.9 |
| TiO ₂ | 0.88 | 0.85 | 0.95 | 0.98 | 0.94 | 0.76 | 0.75 | 0.74 | 0.74 | 0.74 | 0.67 | 1.07 | 0.85 | 0.74 |
| Al ₂ O ₃ | 16.6 | 16.2 | 14.8 | 14.8 | 14.8 | 16.3 | 16.3 | 16.5 | 16.1 | 15.9 | 16.2 | 14.4 | 16.0 | 16.2 |
| Fe ₂ O ₃ | 2.80 | 2.80 | 2.55 | 2.02 | 2.30 | 1.94 | 2.30 | 2.16 | 2.38 | 2.14 | 1.65 | 2.46 | 2.37 | 2.28 |
| FeO | 6.02 | 6.57 | 7.43 | 8.08 | 7.56 | 6.45 | 6.06 | 5.97 | 6.02 | 6.24 | 6.31 | 8.05 | 6.49 | 6.12 |
| MnO | 0.15 | 0.18 | 0.19 | 0.22 | 0.19 | 0.15 | 0.15 | 0.15 | 0.16 | 0.16 | 0.15 | 0.20 | 0.16 | 0.15 |
| MgO | 8.19 | 8.51 | 8.59 | 8.48 | 8.51 | 9.10 | 9.30 | 9.04 | 9.53 | 10.1 | 9.94 | 8.18 | 8.73 | 9.37 |
| CaO | 12.8 | 13.0 | 12.9 | 12.9 | 12.9 | 13.1 | 13.1 | 13.4 | 13.1 | 12.9 | 13.1 | 12.5 | 13.2 | 13.1 |
| Na ₂ O | 2.19 | 1.85 | 1.88 | 2.00 | 1.83 | 1.77 | 1.70 | 1.75 | 1.63 | 1.53 | 1.59 | 2.11 | 1.80 | 1.67 |
| K ₂ O | 0.02 | 0.02 | 0.02 | 0.02 | 0.02 | 0.02 | 0.02 | 0.02 | 0.02 | 0.01 | 0.02 | 0.02 | 0.02 | 0.02 |
| P ₂ O ₅ | 0.06 | 0.06 | 0.06 | 0.07 | 0.06 | 0.06 | 0.06 | 0.05 | 0.05 | 0.05 | 0.05 | 0.07 | 0.06 | 0.05 |
| H ₂ O ⁺ | 1.67 | 1.36 | 1.67 | 1.79 | 1.35 | 1.40 | 1.44 | 1.41 | 1.61 | 1.90 | 1.61 | 1.49 | 1.41 | 1.49 |
| CO ₂ | 0.07 | 0.05 | 0.04 | 0.05 | 0.06 | 0.06 | 0.07 | 0.06 | 0.09 | 0.05 | 0.08 | 0.05 | 0.05 | 0.09 |
| FeS ₂ | — | — | — | — | — | — | — | — | — | — | — | — | — | — |
| Σ | 100.35 | 100.45 | 100.28 | 100.41 | 100.22 | 100.31 | 100.25 | 100.25 | 100.13 | 100.42 | 99.97 | 100.30 | 100.34 | 100.18 |
| Fe ₂ O ₃ ^T | 9.49 | 10.1 | 10.8 | 11.0 | 10.7 | 9.11 | 9.03 | 8.79 | 9.07 | 9.07 | 8.66 | 11.4 | 9.58 | 9.08 |
| S | 0.08 | 0.08 | 0.02 | 0.03 | 0.03 | 0.09 | 0.09 | 0.09 | 0.09 | 0.09 | 0.08 | 0.05 | 0.09 | 0.09 |
| Ox | 0.295 | 0.277 | 0.236 | 0.184 | 0.215 | 0.213 | 0.255 | 0.246 | 0.262 | 0.236 | 0.191 | 0.216 | 0.247 | 0.251 |
| mg _y | 0.668 | 0.663 | 0.650 | 0.642 | 0.650 | 0.700 | 0.706 | 0.706 | 0.710 | 0.722 | 0.728 | 0.626 | 0.680 | 0.706 |
| Trace elements | | | | | | | | | | | | | | |
| K | 81 | n.d. | n.d. | n.d. | 68 | n.d. | n.d. | n.d. | 61 | n.d. | 62 | n.d. | n.d. | n.d. |
| F | n.d. | 70 | n.d. | n.d. | n.d. | 53 | 64 | n.d. | 55 | 53 | 45 | 93 | n.d. | n.d. |
| Cr | 343 | 333 | 305 | 298 | 325 | 378 | 381 | 376 | 372 | 455 | 406 | 178 | 338 | 386 |
| Co | 40 | 41 | 41 | 43 | 43 | 43 | 42 | 39 | 43 | 36 | 43 | 44 | 44 | 37 |
| Ni | 121 | 130 | 90 | 86 | 90 | 149 | 151 | 141 | 170 | 202 | 181 | 78 | 119 | 150 |
| Cu | 84 | 92 | 86 | 87 | 141 | 86 | 85 | 82 | 86 | 89 | 86 | 95 | 85 | 86 |
| Zn | 70 | 64 | 65 | 73 | 65 | 60 | 61 | 56 | 61 | 60 | 54 | 81 | 74 | 60 |
| Ga | 16 | 15 | 16 | 16 | 16 | 14 | 16 | 15 | 13 | 14 | 14 | 16 | 16 | 15 |
| Sr | 70 | 65 | 52 | 52 | 49 | 67 | 64 | 64 | 64 | 60 | 62 | 61 | 65 | 65 |
| Y | 23 | 25 | 27 | 28 | 27 | 22 | 21 | 21 | 21 | 21 | 19 | 29 | 24 | 21 |
| Zr | 59 | 56 | 55 | 58 | 56 | 51 | 50 | 50 | 50 | 48 | 45 | 68 | 55 | 50 |

oxidation because of the high oxidation ability of seawater.

Basalts recovered from the interval between 530 m and 836 m BSF have much lower potassium contents, are less oxidized, and display significantly higher sulfur concentrations. They obviously were altered under suboxic to anoxic conditions by reaction with "evolved" seawater, that is, seawater whose original composition has been changed by reaction with basalts. As is indicated by alteration mineralogy and isotope investigations, this alteration most probably took place at low water/rock ratios and at somewhat elevated temperatures of 60 to 100°C (Alt et al., this volume).

At 836 m BSF, that is, at about the boundary between the pillow section and the transition zone, a pronounced change in type of alteration is to be observed: H₂O⁺ and sulfur contents increase whereas Ox values decrease. All three parameters reach extreme values in the depth interval between 910 and 1059 m BSF. Basalts from this depth interval, which represent the lower portion of the transition zone, display the most spectacular alteration chemistry of all basement rocks recovered from Hole 504B. They are highest in H₂O⁺, show the lowest Ox values, are sometimes extremely enriched in S, Zn, and Cu and exhibit a strong enrichment in manganese. This type of alteration starts at the top of the mineralized stockwork and extends downwards to the boundary between the transition zone and the underlying dike complex.

The bulk-rock manganese and sulfur enrichments together with the highly scattered Zn and Cu contents sug-

gest that the alteration of this basement section, which resulted in conspicuous sulfide deposition, occurred within or near a hydrothermal upflow zone. Such ore precipitations are to be expected where hot metal- and sulfur-rich hydrothermal fluids passing through the crust became oversaturated with respect to sulfides because of changes in temperature and/or compositions. The high manganese contents of the basalts recovered from this basement section are, at least in part, fixed in Mn-rich clay minerals which have been identified among the alteration products (Alt et al., this volume).

Compared to the intensely altered rocks of the transition zone, samples from the underlying dike section appear to be less affected chemically. Two different zones of chemical alteration may be distinguished within the dike sequence, grading more or less continuously into each other. A tentative boundary has been drawn at about 1245 m BSF. In general, H₂O⁺, CO₂, K, and Ox values decrease downward toward the bottom of the hole. Samples from the lowest portion of the hole are very low in potassium (< 100 ppm) and CO₂, display relatively low H₂O⁺ contents of about 1.5 wt. % and have low oxidation ratios ranging from 0.20 to 0.28. Chemically they seem to be less extensively altered than basalts from the upper portion of the dike section.

Although the downhole variation in alteration-sensitive chemical parameters closely reflects the changes established in alteration mineralogy, because of the complexity of the mineral replacements and chemical processes involved we can apply no general correction procedure which would allow a reliable evaluation of the

Table 2. (Continued).

| | | | | | | | | | | | | |
|-----------------|-----------------|-----------------|-----------------|-----------------|---------------|-----------------|-------------------|-----------------|-----------------|-------------------|-----------------|-----------------|
| 130-2, 14-17 | 130-2, 44-58 | 130-3, 78-81 | 131-1, 46-50 | 132-1, 30-34 | 132-2, 3-6 | 133-1, 90-92 | 133-1, 124-128 | 133-2, 25-29 | 134-1, 33-36 | 137-1, 107-109 | 138-1, 48-52 | 141-1, 30-32 |
| 1280.66 | 1281.01 | 1282.80 | 1287.98 | 1295.32 | 1296.55 | 1304.91 | 1305.26 | 1305.77 | 1313.35 | 1328.08 | 1332.50 | 1345.81 |
| 135 | 135 | 135 | 136 | 137 | 137 | 138 | 138 | 138 | 139 | 143 | 144 | 147 |
| 49.0 | 49.1 | 48.5 | 49.0 | 48.8 | 49.0 | 49.7 | 49.5 | 49.5 | 49.4 | 49.0 | 49.7 | 49.3 |
| 0.73 | 0.75 | 0.65 | 0.75 | 0.80 | 0.85 | 0.97 | 0.96 | 0.95 | 0.94 | 0.77 | 0.80 | 0.83 |
| 16.3 | 16.4 | 16.0 | 16.2 | 16.2 | 15.7 | 14.8 | 14.7 | 14.7 | 16.3 | 16.2 | 16.2 | 16.4 |
| 2.10 | 1.97 | 2.20 | 1.94 | 2.19 | 2.33 | 2.66 | 1.95 | 2.37 | 2.51 | 2.31 | 2.10 | 2.40 |
| 6.20 | 6.33 | 5.81 | 6.35 | 6.38 | 6.99 | 7.33 | 7.97 | 7.32 | 6.71 | 6.10 | 6.39 | 6.26 |
| 0.15 | 0.15 | 0.15 | 0.15 | 0.16 | 0.17 | 0.20 | 0.21 | 0.20 | 0.17 | 0.16 | 0.16 | 0.16 |
| 9.39 | 9.12 | 10.5 | 9.36 | 8.82 | 8.65 | 8.42 | 8.45 | 8.44 | 7.68 | 9.38 | 8.77 | 8.33 |
| 13.1 | 13.2 | 12.9 | 13.2 | 13.3 | 13.0 | 13.0 | 12.7 | 12.7 | 12.9 | 13.0 | 13.1 | 13.3 |
| 1.68 | 1.73 | 1.48 | 1.65 | 1.74 | 1.83 | 1.78 | 1.89 | 2.13 | 2.04 | 1.68 | 1.83 | 1.81 |
| 0.02 | 0.01 | 0.02 | 0.02 | 0.02 | 0.02 | 0.02 | 0.02 | 0.02 | 0.02 | 0.02 | 0.02 | 0.02 |
| 0.05 | 0.06 | 0.04 | 0.05 | 0.05 | 0.06 | 0.07 | 0.07 | 0.06 | 0.07 | 0.06 | 0.06 | 0.06 |
| 1.41 | 1.30 | 2.00 | 1.40 | 1.35 | 1.25 | 1.45 | 1.71 | 1.80 | 1.52 | 1.42 | 1.12 | 1.39 |
| 0.05 | 0.13 | 0.07 | 0.06 | 0.06 | 0.06 | 0.05 | 0.04 | 0.05 | 0.06 | 0.07 | 0.05 | 0.07 |
| — | — | — | — | — | — | — | — | — | — | — | — | — |
| 100.18 | 100.25 | 100.32 | 100.13 | 99.87 | 99.91 | 100.45 | 100.17 | 100.24 | 100.32 | 100.17 | 100.30 | 100.33 |
| 8.99 | 9.00 | 8.65 | 8.99 | 9.28 | 10.1 | 10.8 | 10.8 | 10.5 | 9.96 | 9.09 | 9.20 | 9.35 |
| 0.09 | 0.09 | 0.09 | 0.09 | 0.09 | 0.10 | 0.02 | 0.02 | 0.03 | 0.05 | 0.07 | 0.09 | 0.07 |
| 0.234 | 0.219 | 0.254 | 0.216 | 0.236 | 0.231 | 0.246 | 0.181 | 0.226 | 0.252 | 0.254 | 0.228 | 0.257 |
| 0.709 | 0.703 | 0.739 | 0.708 | 0.689 | 0.666 | 0.645 | 0.646 | 0.652 | 0.643 | 0.706 | 0.690 | 0.675 |
| n.d. | 62 | n.d. | n.d. | n.d. | n.d. | 65 | n.d. | n.d. | n.d. | 106 | n.d. | 89 |
| n.d. | 63 | n.d. | n.d. | n.d. | n.d. | 73 | n.d. | n.d. | n.d. | n.d. | 70 | n.d. |
| 377 | 373 | 456 | 386 | 369 | 349 | 291 | 288 | 292 | 210 | 398 | 355 | 340 |
| 41 | 40 | 46 | 40 | 43 | 48 | 41 | 47 | 43 | 37 | 43 | 46 | 38 |
| 156 | 145 | 213 | 152 | 133 | 121 | 85 | 87 | 84 | 89 | 164 | 118 | 107 |
| 86 | 84 | 83 | 87 | 85 | 98 | 101 | 100 | 148 | 77 | 85 | 79 | 82 |
| 56 | 58 | 55 | 57 | 68 | 64 | 73 | 75 | 72 | 69 | 64 | 64 | 65 |
| 14 | 15 | 14 | 15 | 14 | 15 | 16 | 15 | 16 | 17 | 15 | 16 | 15 |
| 65 | 66 | 58 | 64 | 66 | 63 | 49 | 50 | 53 | 65 | 63 | 65 | 62 |
| 21 | 21 | 18 | 21 | 23 | 26 | 27 | 27 | 27 | 25 | 22 | 21 | 23 |
| 50 | 51 | 45 | 51 | 53 | 57 | 57 | 57 | 56 | 59 | 52 | 51 | 53 |

Table 3. Rare earth element (REE) abundances of selected Leg 83 basalt samples from Hole 504B.

| REE | 72-1, 74-76 | 80-1, 38-41 | 83-1, 70-73 | 87-2, 37-40 | 88-1, 111-115 | 93-3, 21-25 | 95-1, 140-143 | 103-1, 92-95 | 129-1, 3-7 |
|-----|----------------|----------------|----------------|----------------|------------------|----------------|------------------|-----------------|---------------|
| La | 0.96 | 0.82 | 0.72 | 2.7 | 3.0 | 3.7 | 1.3 | 1.1 | 1.0 |
| Ce | 4.4 | 3.6 | 2.7 | 8.0 | 8.2 | 13.7 | 4.7 | 4.0 | 3.6 |
| Pr | 0.28 | 0.66 | 0.76 | 1.8 | 1.5 | 2.7 | 1.3 | 0.82 | 0.56 |
| Nd | 5.0 | 4.6 | 3.1 | 6.2 | 7.1 | 12.6 | 5.8 | 4.8 | 4.0 |
| Sm | 3.2 | 1.8 | 1.5 | 2.5 | 2.1 | 2.7 | n.d. | 2.1 | 1.5 |
| Eu | 1.1 | 0.73 | 0.54 | 0.90 | 0.92 | 0.96 | 0.84 | 0.74 | 0.70 |
| Gd | 3.4 | 2.9 | 2.1 | 3.4 | 3.2 | 5.8 | 3.1 | 3.1 | 2.8 |
| Tb | 0.66 | 0.50 | 0.46 | 0.62 | 0.50 | 0.86 | 0.48 | 0.40 | 0.58 |
| Dy | 3.8 | 3.7 | 2.7 | 3.8 | 4.3 | 5.9 | 4.4 | 4.1 | 3.3 |
| Ho | 0.88 | 0.88 | 0.56 | 0.78 | 1.1 | 1.2 | 0.86 | 0.86 | 0.73 |
| Er | 2.5 | 2.5 | 1.7 | 2.4 | 3.0 | 3.6 | 2.7 | 2.7 | 2.2 |
| Yb | 2.6 | 2.5 | 1.8 | 2.3 | 2.7 | 3.4 | 2.4 | 2.6 | 2.2 |
| Lu | 0.34 | 0.26 | 0.28 | 0.32 | n.d. | 0.25 | 0.30 | 0.32 | 0.14 |

Note: Column heads give core-section, interval (in cm) for Hole 504B samples.

original major oxide composition of the rocks. This holds especially true for the Leg 83 samples, which are more intensely altered than the Legs 69 and 70 samples. According to Alt and Emmermann (this volume), Leg 83 rocks exhibit trends toward loss of SiO₂, CaO, gain of Na₂O, H₂O, and variable changes in Al₂O₃ and MgO.

This conclusion appears to be substantiated by plots of Na₂O, CaO, and SiO₂ versus H₂O⁺ for the least altered Leg 83 samples selected for the present study (Fig. 5). As is to be seen from Figure 5, Na₂O contents display in general a slight increase with increasing H₂O⁺, despite a considerable scatter, whereas CaO and, less regularly, SiO₂ decrease concomitantly. In contrast, nei-

ther Al₂O₃ nor MgO exhibit systematic changes with varying H₂O⁺ in the samples.

However, even if a recalculation of the major oxides to a dry and reduced state and a normalization to 100% is quite obviously not adequate for deriving the exact primary chemistry of the Leg 83 samples, this procedure provides at least a qualitative estimate of their original composition and allows direct comparison with the glass data published by Natland et al. (1983). Figure 6 shows in a series of histograms the major oxide frequencies of 56 basalt glasses that were sampled from the volcanic section down to 800 m BSF, 112 least altered basalts from throughout the volcanic section, and 85 samples

Table 4. Average composition of 58 least altered basalts and 51 fresh basaltic glasses from the Leg 70 section of Hole 504B.

| | Leg 70 basalts (average $\pm 1\sigma$) | | Basaltic glasses (average $\pm 1\sigma$) | |
|--------------------------------|--|------|--|------|
| SiO ₂ | 50.06 | 0.45 | 50.66 | 0.66 |
| TiO ₂ | 0.94 | 0.09 | 0.97 | 0.07 |
| Al ₂ O ₃ | 15.43 | 0.59 | 14.96 | 0.64 |
| Fe ₂ O ₃ | 2.98 | 0.59 | 1.65 ^a | 0.07 |
| FeO | 6.65 | 0.67 | 8.42 ^a | 0.36 |
| MgO | 8.44 | 0.38 | 8.20 | 0.34 |
| CaO | 12.94 | 0.43 | 12.78 | 0.24 |
| Na ₂ O | 2.19 | 0.30 | 2.00 | 0.15 |
| K ₂ O | 0.02 | 0.01 | 0.03 | 0.01 |
| P ₂ O ₅ | 0.07 | 0.01 | 0.08 | 0.01 |

^a Assuming $\text{Fe}^{3+}/\text{Fe}^{\text{T}} = 0.15$.

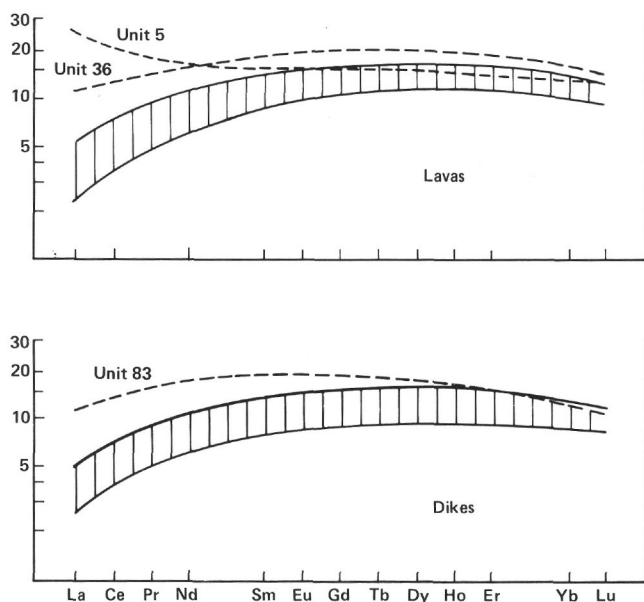


Figure 2. Chondrite-normalized rare earth element distribution patterns of Hole 504B lavas and dikes.

from the dike section of the hole. According to their lithostratigraphic provenance, samples from the transition zone were allocated either to the lavas or to the dikes.

As is evident from this comparison, the dike basalts are very similar to the basalts of the volcanic layer in major oxide chemistry and cover almost the same range of variation as the basalt glasses. Altogether, the chemical spectrum of the dike samples appears to be slightly displaced toward more MgO-rich basalt types. However, there is no indication that the higher MgO contents, which are up to 10.5 wt.%, might be due to secondary Mg-uptake from Mg-enriched alteration fluids. The very pronounced negative correlation between the TiO₂ contents and the mg-values, which is even greater than for the lavas and the basalt glasses (Fig. 7), rather favors the assumption that more primitive, that is, less evolved chemical types were recovered from the dike section.

As was the case for the volcanic section, a few samples were cored from the dike section that differ markedly from the majority of the rocks in that their TiO₂ contents at similar mg-values are significantly higher. Those samples which represent Lithologic Unit 83 are also enriched in Na₂O and P₂O₅ and greatly resemble the exceptional basalt types of Lithologic Units 5 and 36. Accordingly, Unit 83 basalts are distinguished from all other basalts recovered from the Leg 83 portion of the hole by higher abundances and different ratios of hygromagmaphile trace elements as well. This feature is clearly documented in Figures 7 to 9. The LREE contents of Unit 83 basalts are, by a factor of 2–3, higher than those of the majority of the rocks, which are extremely low in LREE and exhibit chondrite-normalized REE distribution patterns that lie within the boundaries shown in Figure 2. The La/Sm enrichment factors (e.f.) of the two basalt types are 0.66 and 0.37, respectively.

Similarly, Zr and F, and to a lesser degree Y and Sr, are enriched in Unit 83 basalts (Fig. 8). In plots of Y versus Zr and Zr versus TiO₂ (Fig. 9), Unit 83 samples are sharply set off from the majority of the basalts, which display rather regular chemical variations and are arranged on well-defined trend lines. Since Ti, Zr, and Y are both relatively incompatible and alteration-resistant, these elements provide the best indicators of the primary chemical features of the basalts and are most suited to elucidating the chemical relations between the rocks recovered. Thus, from these diagrams, two statements seem to be substantiated:

1. The majority of the Leg 83 samples are closely related chemically and may be considered as differentiation products of a common parental magma. The very systematic variations observed can be plausibly explained as result of limited crystal fractionation operative in a high-level magma chamber.

2. Unit 83 basalts and all other basalts recovered from the Leg 83 portion of the hole cannot be related by fractionation processes. The marked differences in hygromagmaphile element abundances and ratios at similar mg-values indicate the existence of two different parental magmas. Furthermore, the significant deviation of a few samples from the general fractionation path by element ratios intermediate between those of the majority of the basalts and Unit 83 samples might reflect some kind of mixing between the two magma types.

Whereas Ti, Zr, and Y still represent primary igneous abundances, as is suggested by the good positive correlations between these elements, Sr contents in many samples have been modified by secondary processes. This is clearly demonstrated by a plot of Sr versus Zr which exhibits a considerable scatter (Fig. 8). On the other hand, fluorine appears to be more alteration-resistant and might even have retained its original abundances.

SUMMARY OF RESULTS AND CONCLUSIONS

DSDP Hole 504B penetrates 1075.5 m into the oceanic basement through a 571.5 m lava pile and a 209 m transition zone made up of lavas and dikes into 295 m of a sheeted dike complex. The pillow lavas and dikes are re-

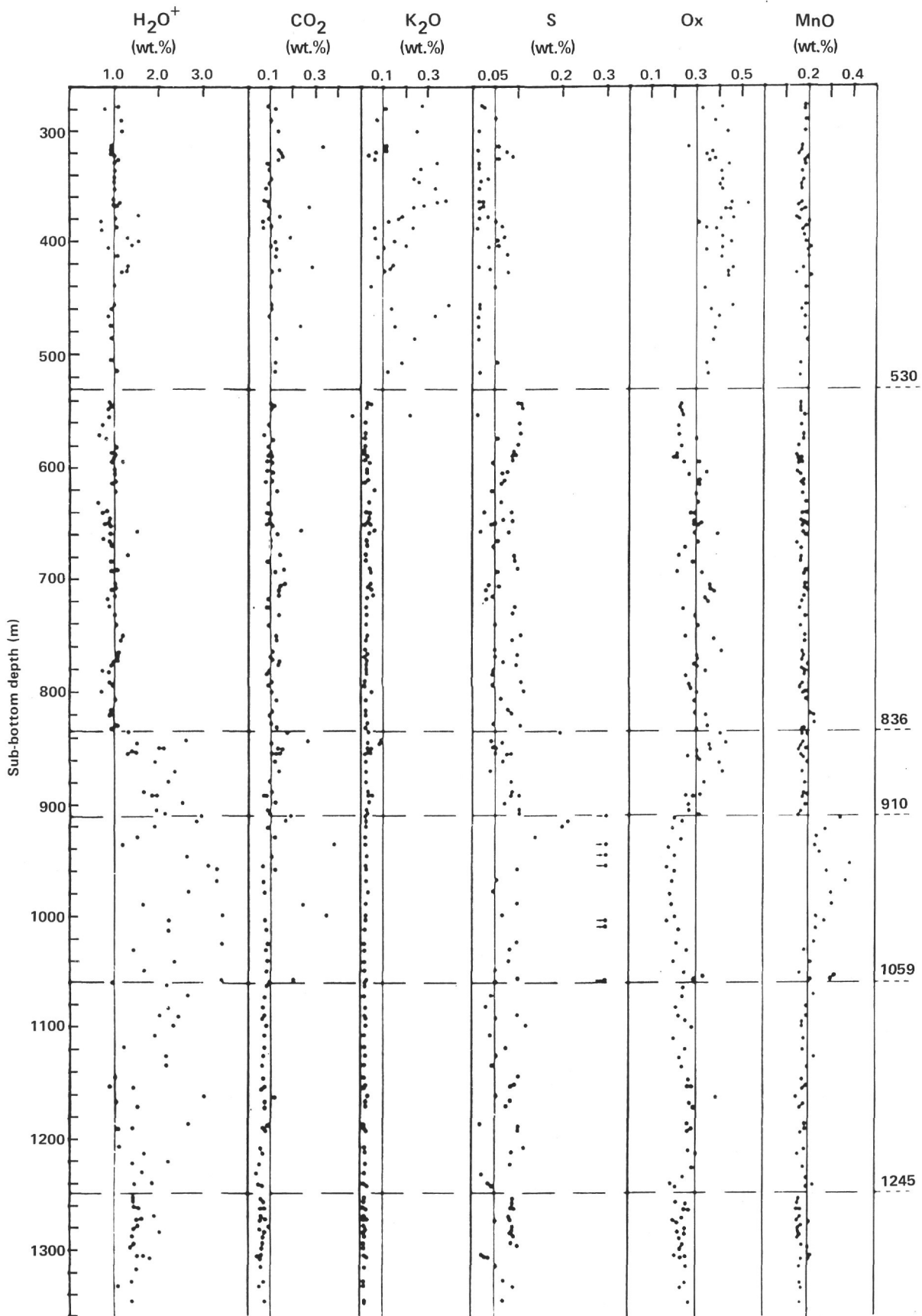


Figure 3. Downhole variation in alteration-sensitive chemical parameters of 194 least altered basalts from the Legs 69, 70, and 83 sections of Hole 504B.

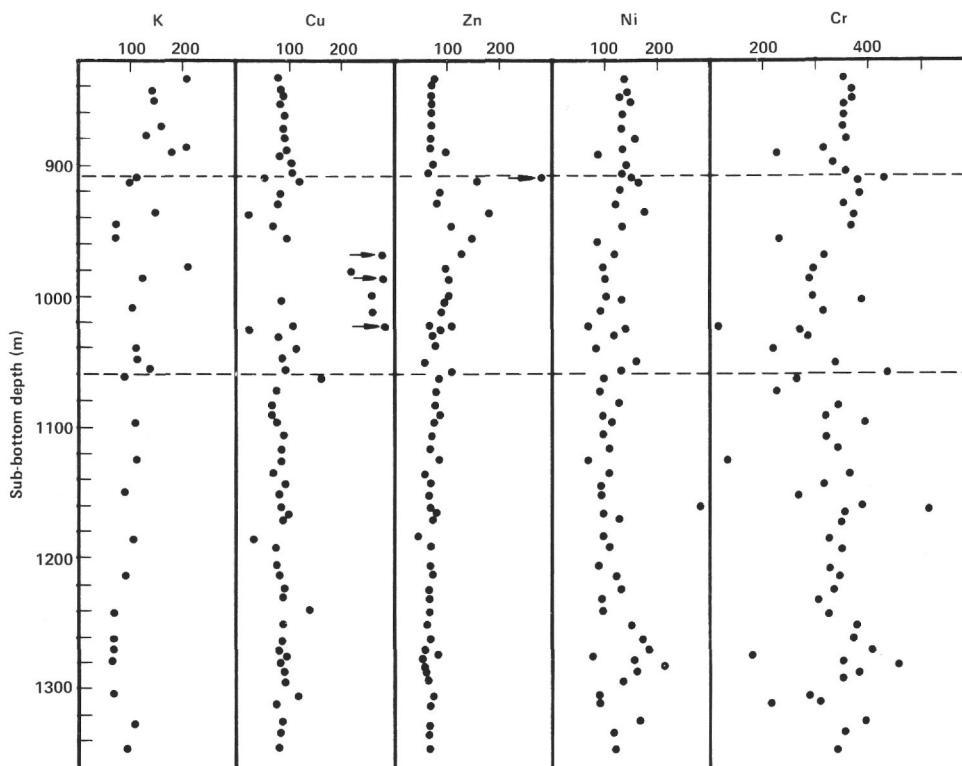


Figure 4. Downhole variation (in ppm) of some selected trace elements in Leg 83 basalts.

markably uniform and consist predominantly of fine- to medium-grained plagioclase-olivine \pm clinopyroxene \pm chrome spinel phryic basalts with aphyric types becoming more abundant with depth. All rocks recovered from Hole 504B are mineralogically and chemically altered to some extent. Detailed studies of the downhole variation of secondary minerals and mineral assemblages documented the existence of three major, depth-related, alteration zones which are separated by relatively sharp boundaries: (1) an upper alteration zone (from 274.5 to 584.5 m BSF) displaying the typical effects of "seafloor weathering," (2) a lower alteration zone (from 584.5 to 836 m BSF) that was presumably produced by interaction of low-temperature reducing solutions at low water/rock ratios, and (3) a high-temperature alteration zone comprising most of the transition zone and the dike section (from 898 m to the bottom of the hole). The latter revealed the first *in situ* ocean floor basalts containing greenschist-facies alteration minerals. The pronounced changes in alteration mineralogy observed within the depth range from 836 to 898 m BSF, that is, between the second and third alteration zone, might be interpreted as the result of a steep temperature gradient from low-temperature ($\leq 100^\circ\text{C}$) alteration solutions circulating in the lava pile to higher temperature fluids which affected the lower portion of the basement (Alt et al., this volume).

The mineralogically defined alteration zones are nicely reflected in very systematic changes of alteration chemistry with depth. Among the components determined, the contents of H_2O^+ , CO_2 , sulfur, potassium, manganese, zinc, and copper as well as the iron oxidation ratio

proved to be the most sensitive chemical indicators of alteration. Downhole variation of these parameters which were measured on 194 least altered whole-rock samples, denote five distinct and sharply delimited alteration zones. Alteration in the uppermost portion of the volcanic section (from 274.5 to 530 m BSF) clearly exhibits the effects of reaction of the lavas with cold, oxygenated seawater. This is indicated by a considerable potassium uptake, a marked iron oxidation, and sulfur loss through sulfide oxidation. The underlying second alteration zone, which extends from 530 to 836 m BSF, does not show any striking chemical effects. It is characterized by low and uniform contents of H_2O^+ (~ 1 wt. %), CO_2 (~ 0.10 wt. %), K (~ 200 ppm), significantly higher sulfur concentrations (~ 800 ppm), and a lower iron oxidation ratio. These chemical findings are in good agreement with the interpretation, based on the alteration mineralogy, that alteration within this basement portion occurred under suboxic to anoxic conditions, either with seawater at low water/rock ratios or with seawater that had previously reacted with basalts (Alt et al., this volume).

In the depth range from 836 to 910 m BSF a major change in the alteration regime is indicated by a strong downhole increase in H_2O^+ and a concomitant decrease of the iron oxidation ratio. This "transitional" zone is underlain by a very distinctive chemical alteration zone that extends from 910 m to 1059 m BSF. Its upper boundary coincides with the top of a stockwork-like sulfide mineralization, whereas its lower boundary is close to the beginning of the dike section of the hole. Alteration within this zone is intense and took place under strongly

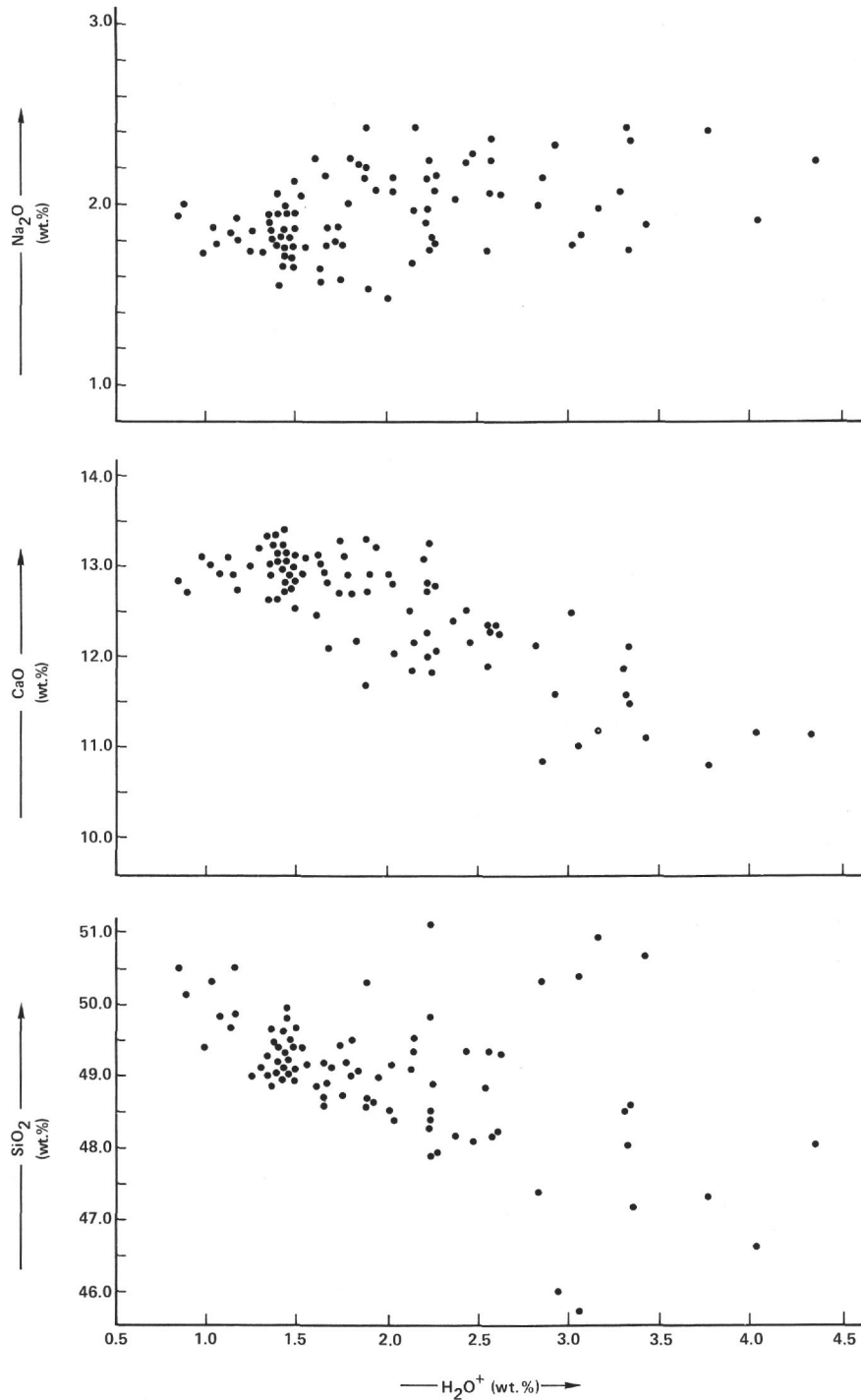


Figure 5. Alteration plot of least altered Leg 83 basalts using H_2O^+ as an index of the degree of alteration.

reducing conditions, as is demonstrated by an extremely low degree of iron oxidation. The rocks recovered display the highest H_2O^+ contents, a conspicuous manganese enrichment and highly scattered abundances of sulfur, zinc, and copper. Altogether, these spectacular chemical alteration effects clearly show that this basement portion was affected by highly reducing Mn-, Zn-, Cu-, and S-enriched hydrothermal fluids and thus strongly

support the conclusion that this zone was at one time within or near a hydrothermal upflow zone. Ore precipitation of the kind observed within the stockwork zone requires oversaturation of a hydrothermal solution with respect to Zn, Cu, (Fe, Pb) sulfides. Since temperature and composition are the most important factors controlling the solubility of metal sulfides, such ore precipitations are expected to occur where the hydrothermal fluids came

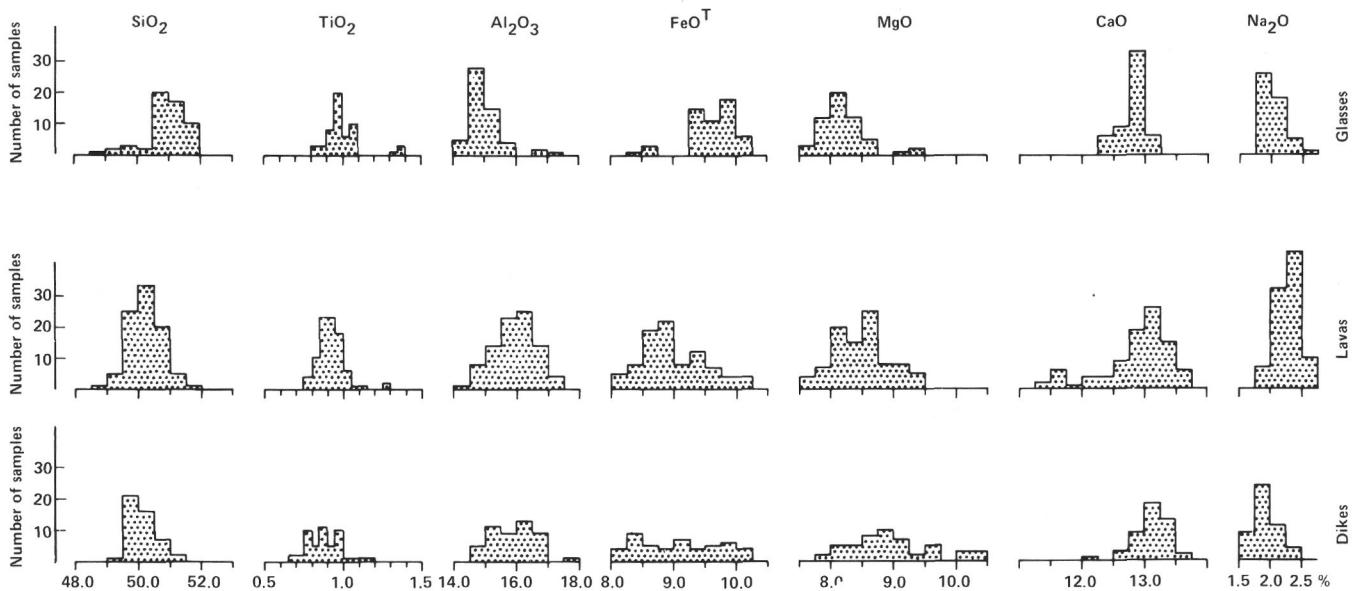


Figure 6. Major oxide frequencies of basalt glasses, lavas, and dikes from Hole 504B.

into contact with solutions lower in temperature and/or with lower concentrations of complexing anions.

The very different regimes of chemical alteration traceable in the volcanic section and the underlying basement portion and the rapid change in alteration chemistry from 836 to 910 m BSF suggest that this crustal interval represents a former zone of mixing of upflowing hydrothermal fluids and lower temperature solutions (seawater or evolved seawater, respectively) circulating in the lava pile. However, the present chemical data do not allow resolution of whether this mixing took place beneath the now existing 571-m lava pile or occurred close to the surface (subsurface mixing) of a volcanic layer that was then thinner.

Despite the effects of alteration on the basalt chemistry, reliable conclusions can be drawn about the original composition and variation of the basement rocks recovered from this site. Of special importance in evaluating the major oxide data of lavas and dikes are the analyses of fresh basaltic glasses, sampled throughout the lava pile, that define unaltered rock compositions and thus provide a suitable base for comparison. Among the minor and trace elements Ti, Zr, and Y provided to be the most reliable indicators of the primary chemical features of the rocks.

Summing up all chemical results obtained by whole-rock analyses of least altered samples:

1. Lavas and dikes are rather uniform in composition and cover almost the same range of variation. However, in general, the compositional spectrum of the dike basalts appears to be somewhat extended toward more primitive, i.e., MgO-rich, varieties. A specific feature of all Hole 504B basement rocks is their high MgO-contents (up to 10.5 wt.%) and their extremely low K-contents, which are around 200 ppm. According to their normative mineralogies all samples analyzed classify as olivine tholeiites. Their mg-values range from 0.60 to 0.74, indicating that the respective magmas experienced

only a very limited degree of crystal fractionation prior to their eruption or intrusion.

2. Despite the general compositional similarity of the rocks, two major basalt groups were found in both the lavas and the dikes. These two groups exhibit significantly different abundances of incompatible elements and are to be distinguished in their major oxide chemistry by different contents of Na₂O, TiO₂, and P₂O₅ at similar mg-values.

The majority of the basalts from the lava and dike section of the hole display low contents of Na₂O (1.5–2.2 wt.%), TiO₂ (0.6–1.2 wt.%), and P₂O₅ (0.04–0.10 wt.%) and are characterized by very low contents of hygromagmaphile elements (Sr, 42–80 ppm; Y, 18–30 ppm; Zr, 38–83 ppm; La, 0.7–3.0). In fact, these rocks are among the most depleted basalts recovered so far from the ocean floor. Interdigitated with this basalt type is a very rarely occurring basalt type that is distinctly higher in Na₂O (2.4 wt.%), TiO₂ (1.5 wt.%), and P₂O₅ (0.18 wt.%) and much less depleted in hygromagmaphile elements (Sr, 85 ppm; Zr, 140 ppm; Y, 35 ppm, La, 3.7 ppm). The latter was found to be restricted to Lithologic Units 5 and 36 of the lava section and Lithologic Unit 83 of the dike section.

3. The majority of the basalts are chemically closely related and most probably represent differentiation products of a common parental magma. The compositional variability observed within this basalt group follows rather regular chemical patterns that can be plausibly explained as a result of limited high-level crystal fractionation. This conclusion is especially substantiated by well-defined trend lines in plots of incompatible, alteration-resistant elements. Assuming that the composition of the least-evolved basalts of this group in a first approximation corresponds to the composition of the parental melt, then the chemical features of this melt were about the following (wt.%): SiO₂, 49%; TiO₂, 0.65%; Al₂O₃, 16.3; FeO^T, 7.8%; MnO, 0.15%; MgO, 10.0%;

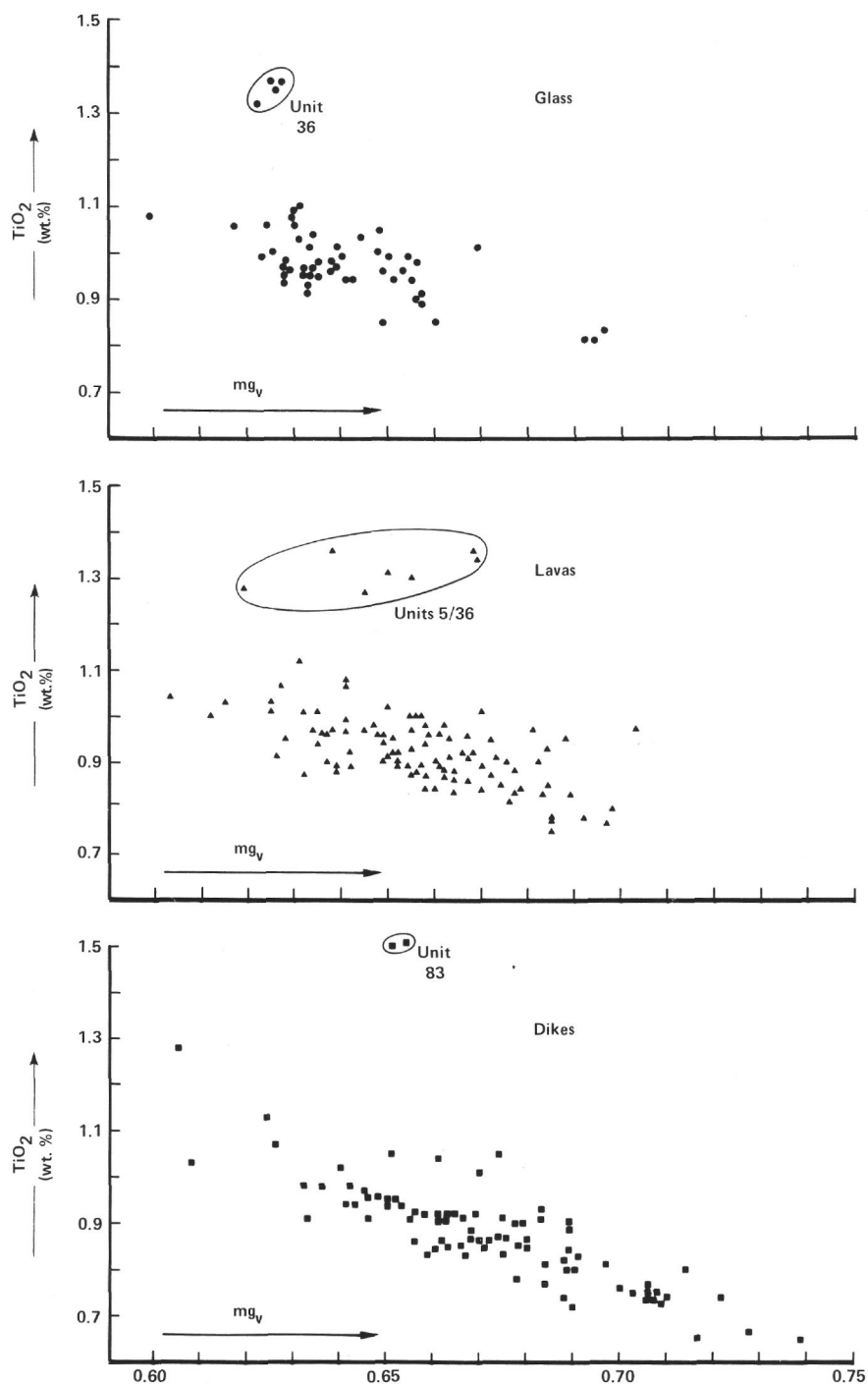


Figure 7. Plots of TiO_2 versus mg -values (mg_v) of basalt glasses, lavas, and dikes from Hole 504B.

mg -value 0.73; CaO , 13.0%; Na_2O , 1.5%; K_2O , 0.02%; P_2O_5 , 0.05%; Cr , 450 ppm; Ni , 200 ppm; Sr , 55 ppm; Y , 20 ppm; Zr , 45 ppm.

4. The two basalt groups are not comagmatic, but rather have to be regarded as differentiation products of two different parental magmas. This conclusion is based on the fact that the rarely occurring basalt type, because of different ratios in the abundances of its hygromagmaphile elements, clearly plots outside the general frac-

tionation path as defined by the majority of the basalts. However, there is evidence that at least occasionally some kind of mixing between the two magma types took place.

5. The multiple eruptions and intrusions of compositionally almost identical magma batches indicate that the magma chamber beneath the Costa Rica Rift from which these melts were released had reached nearly steady-state conditions. The presence of lavas and dikes that crystallized from a distinctly different parental melt, on

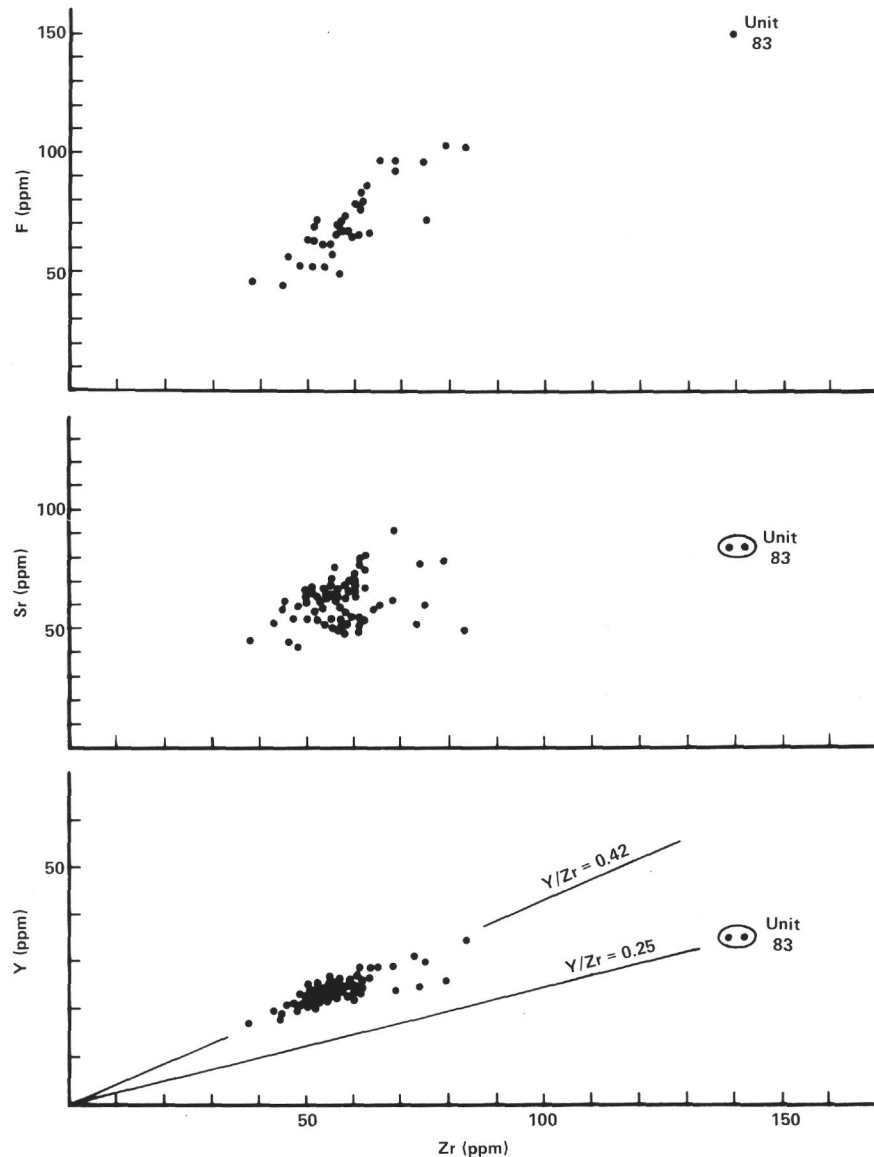


Figure 8. Plots of F, Sr, and Y versus Zr for Leg 83 basalts.

the other hand, requires the existence of a separate or at least not completely interconnected conduit-magma chamber system for this magma type.

6. The occurrence of two different magma types suggests that there was some chemical heterogeneity in the mantle source underlying the CRR. The majority of the basalts crystallized from melts that were derived from an extremely depleted mantle source. The rarely occurring magma type might have originated from relict pockets of less depleted mantle material or from a depleted mantle source that was affected by addition of metasomatic fluids.

ACKNOWLEDGMENTS

I am very grateful to Dr. J. Erzinger, Mrs. M. Grünhäuser, and Mrs. B. Garcia for their assistance in performing the chemical analyses. I also wish to thank Mrs. R. Helmig for the preparation of the figures. This research was supported by the Deutsche Forschungsgemeinschaft (grant Em 23/8-9).

REFERENCES

- Abbey, S., 1980. Studies in "standard samples" for use in the general analysis of silicate rocks and minerals. *Geostandards Newsl.*, 4(2): 163-190.
- , 1982. An evaluation of USGS III. *Geostandards Newsl.*, 6(1):47-76.
- Anderson, R. N., Honnorez, J., Becker, K., Adamson, A. C., Alt, J. C., Emmermann, R., Kempton, P. D., Kinoshita, H., Laverne, C., Mottl, M. J., and Newmark, R. L., 1982. DSDP Hole 504B, the first reference section over 1 km through Layer 2 of the oceanic crust. *Nature*, 300:589-594.
- Becker, K., Von Herzen, R. P., Francis, T. J. G., Anderson, R. N., Honnorez, J., Adamson, A. C., Alt, J. C., Emmermann, R., Kempton, P. D., Kinoshita, H., Laverne, C., Mottl, M. J., and Newmark, R. L., 1982. *In situ* electrical resistivity and bulk porosity of the oceanic crust, Costa Rica Rift. *Nature*, 300:594-598.
- Erzinger, J., Heinschild, H. J., and Stroh, A., in press. *Bestimmung der Seltenen Erden in Gesteinen mit der ICP-AES*. Weinheim (Verlag Chemie).
- Gladney, E., 1983. 1982 Compilation of elemental concentrations in eleven United States Geological Survey rock standards. *Geostandards Newsl.*, 7(1):3-226.

Honnorez, J., Laverne, C., Hubberten, H.-W., Emmermann, R., and Muehlenbachs, K., 1983. Alteration processes in Layer 2 basalts from Deep Sea Drilling Project Hole 504B, Costa Rica Rift. *In* Cann, J. R., Langseth, M. G., Honnorez, J., Von Herzen, R. P., White, S. M., et al., *Init. Repts. DSDP, 70*: Washington (U.S. Govt. Printing Office), 509-550.

Hubberten, H.-W., Emmermann, R., and Puchelt, H., 1983. Geochemistry of basalts from Costa Rica Rift Sites 504 and 505 (Deep Sea Drilling Project Legs 69 and 70). *In* Cann, J. R., Langseth, M. G., Honnorez, J., Von Herzen, R. P., White, S. M., et al., *Init. Repts. DSDP, 70*: Washington (U.S. Govt. Printing Office), 791-803.

Marsh, N. G., Tarney, J., and Hendry, G. L., 1983. Trace element geochemistry of basalts from Hole 504B, Panama Basin, Deep Sea

Drilling Project Legs 69 and 70. *In* Cann, J. R., Langseth, M. G., Honnorez, J., Von Herzen, R. P., White, S. M., et al., *Init. Repts. DSDP, 70*: Washington (U.S. Govt. Printing Office), 747-763.

Natland, J. H., Adamson, A. C., Laverne, C., Melson, W. G., and O'Hearn, T., 1983. A compositionally nearly steady-state magma chamber at the Costa Rica Rift: Evidence from basalt glass and mineral data, Deep Sea Drilling Project Sites 501, 504, and 505. *In* Cann, J. R., Langseth, M. G., Honnorez, J., Von Herzen, R. P., White, S. M., et al., *Init. Repts. DSDP, 70*: Washington (U.S. Govt. Printing Office), 811-858.

Date of Initial Receipt: 16 January 1984

Date of Acceptance: 5 March 1984

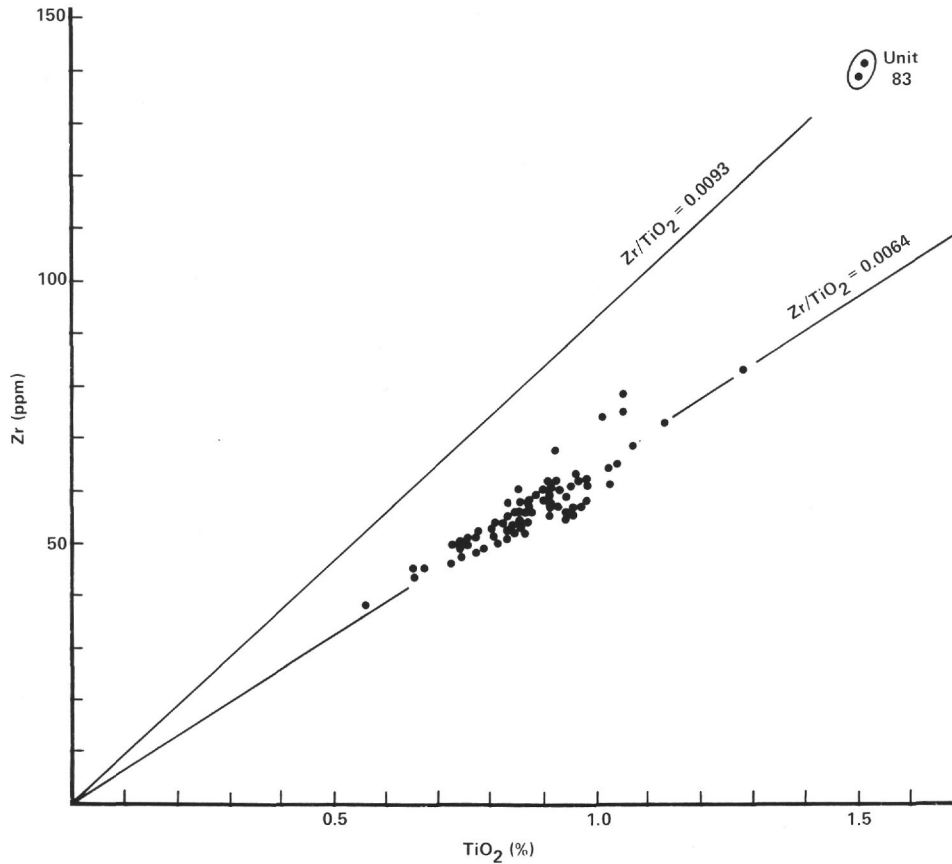


Figure 9. Plot of Zr versus TiO_2 for Leg 83 basalts.